ISSN: 2664-9640

Analysis and Research on Vibration Fatigue Fracture of Crude Oil Turbine Governor Bracket

Zhenghao Cheng, Hao Yu, Qiang Gu, Yaohua He

CNOOC (China) Co., Ltd. Zhanjiang Branch, China

Abstract

The mechanical structure will be subjected to cyclic stress during the working process. Under certain circumstances, the mechanical structure will suffer fatigue damage under the action of cyclic stress. For example, the failure of the restraint of the component will cause it to appear unstable and under the action of cyclic stress Fatigue tearing will occur under different conditions. In order to explore the reason for the fracture of the connection of the crude oil engine governor bracket, the finite element analysis method is used to explore the stress distribution of the bracket under different constraints, and the fracture position of the bracket is determined by combining the buckling factor under the unstable state. Stiffeners are added to reduce the risk of fracture at the joint of the support after restraint failure. The influence of design parameters such as the height, length and thickness of the stiffener on the stress distribution at the joint of the support, the buckling factor of the support and the stress of the stiffener are analyzed. The optimal scheme of rib design guides the selection of reinforcement rib on site.

Keywords

Crude oil engine governor bracket connection; finite element method; buckling factor.

1. Introduction

An offshore platform uses two Shaanxi Diesel 12-cylinder crude oil generators, each with a power of 5600KW, which plays an important role in ensuring the safe production of the platform.

The governor bracket of the crude oil generator mainly plays the role of installing the debugger and fixing the exhaust baffle. Due to the vibration characteristics of the crude oil generator itself, the bottom of the bracket is broken, which affects the stability of its speed regulation. The normal operation of the crude oil machine is of great significance.

The vibration of mechanical structures widely exists in various fields of mechanical engineering. How to improve the anti-vibration capability of mechanical structures, how to prevent the resonance generated by the system, and the problem of vibration balance caused by unbalanced forces, all need to be discussed in depth. This paper Vibration yield fracture of CNPC generator support is one of the problems of mechanical vibration, and it is also a common form of fatigue damage in mechanical structures. Mechanical fatigue is mainly divided into high cycle fatigue, that is, mechanical vibration under the action of low cyclic stress, At this time, elastic strain dominates; while low-cycle fatigue is the mechanical vibration caused by high cyclic stress, and plastic strain dominates.

Mechanical vibration is a special form of exercise, in the process of this movement stents around its equilibrium position as a movement back and forth, the cycle of repeated movement will inevitably cause mechanical circulating stress, as the cycle number and the accumulation of time, will inevitably produce tiny cracks, the fatigue life of the third order theory [1], in under the action of cyclic stress mechanism, The mechanical structure support will go through three stages, as shown in Figure 1.

ISSN: 2664-9640

No crack stage. Although there is accumulation of mechanical cyclic stress in this stage, these cyclic stresses cannot achieve the result of crack;

In the stage of small crack, small cracks gradually occur in the structure after enough cyclic mechanical stress is accumulated. In the figure, a_{sml} is the upper limit size of small crack, a_{sml} is the lower limit size of small crack, and $a_0$is the size of engineering crack, but these cracks are not enough to make the structure fail.

Along with the mechanical structure under the effect of cyclic vibration stress of continuous, the crack size will gradually over asmu into a large crack stage, at this time of the crack can be observed by the naked eye, when the big crack extension to acr, mechanical structure will be destroyed, lost its original function, which is needed for analysis of mechanical parts in the design to avoid, Among them, small cracks and large cracks are collectively referred to as crack growth life, and the time experienced by the three stages is collectively referred to as the whole life of mechanical parts [2].

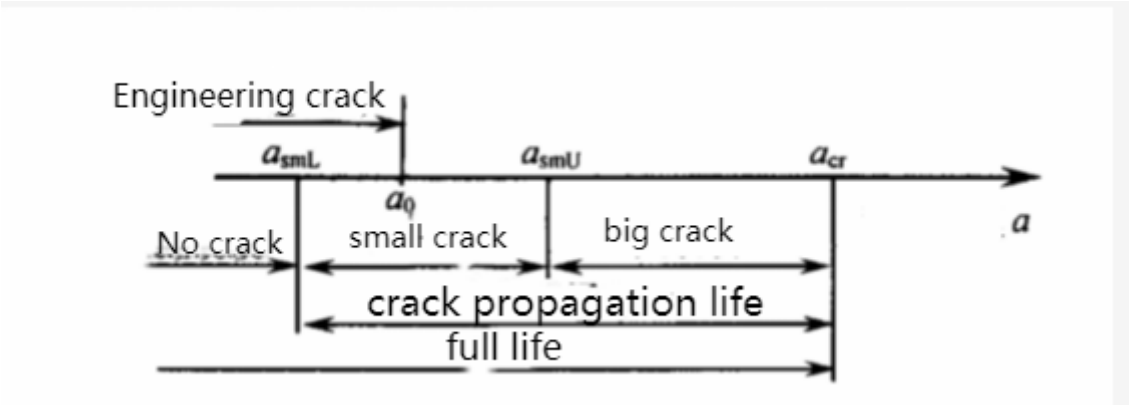

Figure1: Fatigue crack life diagram of mechanical structure

The earliest record of fatigue analysis was completed by Albert[3], a German mining engineer, in 1829. He repeatedly loaded loads on the elevator chain in the mine and checked the reliability of the chain after several cycles. In 1843, Rankine[4], a British railway engineer, noticed that there was stress concentration in mechanical parts and made a certain study on it, thus obtaining a new understanding of fatigue fracture characteristics. From 1852 to 1869, Wohler [5] made a new study on fatigue failure. After applying continuous cyclic loads to railway tracks, he found that their load capacity was far lower than that of static loads. He proposed the method of describing fatigue behavior by S-N curve and proposed the concept of "fatigue endurance limit". In 1874, Gerber[6], a German engineer, proposed a method to consider the influence of average stress on life. In 1937, Neuber[7] pointed out that the average stress at the root of notch with stress concentration was more representative of the severity of load than the peak stress, and Miner[8] in the same year proposed the fatigue linear cumulative damage theory, and then the local stress strain method was gradually formed.

The fracture of the governor support of crude oil generator is shown in Figure 2, where fatigue fracture occurs at the stress concentration position of the support. Based on this, this paper takes the turbine air duct support of crude oil generator as the research object. Under the condition of considering the cyclic vibration stress, the vibration fatigue analysis of the support is carried out, and the reinforcement is set at the fracture position to improve the vibration resistance ability of the mechanical structure.

ISSN: 2664-9640

Figure2: Fracture site of governor support of crude oil generator

2. Basic Theory

The statics equation of the support is:

$$MX_1+CX_2+KX_3=F(t) \quad (1)$$

In the formula:

M -- the mass matrix

C -- damping matrix

K -- system stiffness matrix

F-- the system is under load

X1,X2,X3 -- the acceleration, the velocity, and the displacement of the system

The harmonic response motion equation of the scaffold is:

$$F=\{F_{Max}e^{iq}\}e^{iwt}= (\{F_1\}+i\{F_2\}) e^{iwt} \quad (2)$$

$$u=\{u_{Max}e^{iq}\}e^{iwt}= (\{u_1\}+i\{u_2\}) e^{iwt} \quad (3)$$

In the formula:

F_{Max}--amplitude of vibration stress

U_{Max}- displacement amplitude

F_1 and F_2--real and imaginary parts of vibrational stress

u_1 and u_2--the real and imaginary parts of the displacement

q--phase Angle of the stress function

The buckling equation of the scaffold is:

$$([K]+Y_1[S]) \{Q_1\}=0 \quad (4)$$

In the formula:

K -- system stiffness matrix

S -- system strain

Y_1 -- buckling load factor

Q_1 -- buckling mode

ISSN: 2664-9640

3. Establishment of numerical model

The crude oil generator governor support model studied in this paper is shown in Figure 3. It can be seen from the figure that the support is mainly connected with the crude oil generator by four fixed points, namely, the two bolt connection plates of the upper constraint, the middle constraint bolt connection plate, the lower constraint bolt connection plate, and the bottom constraint connected with the cover plate of the crude oil generator rotor.

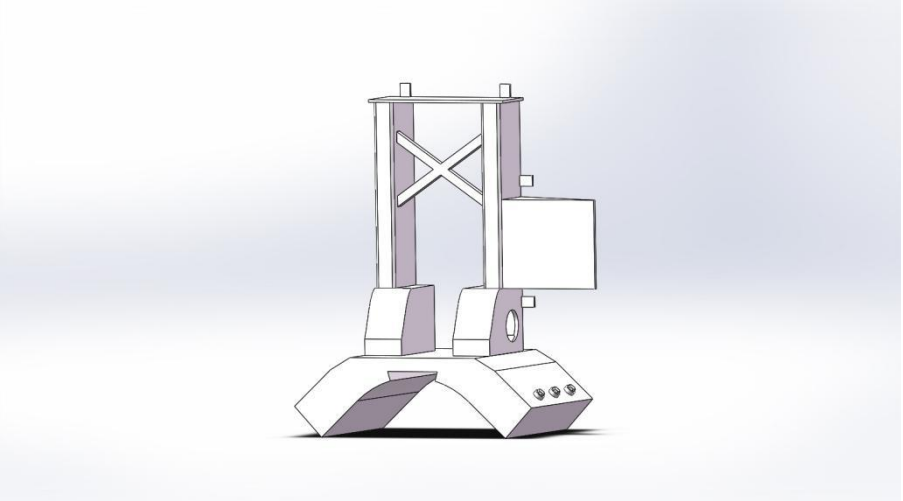

Figure 3: The crude oil generator governor support model

The frequency of the crude oil generator was 50Hz, and the vibration accelerations in X, Y and Z directions at the crack were 70mm/ s2, 10mm/ s2 and 22.8mm/ s2, according to the vibration meter.

4. Failure cause analysis

By the situation of feedback can preliminary judgment to support the cause of the failure due to vibration in bolt connection plate lay off, leading to the bottom of the bracket is circulating mechanical stress, fatigue failure, in order to prove the accuracy of the conjecture, this paper uses ANSYS finite element analysis of the model, the constraint conditions can be divided into the following eight kinds, respectively is: (1) The full constraint does not fail, (2) the full constraint fails, (3) the upper constraint fails, (4) the middle constraint fails, (5) the lower constraint fails, (6) the upper and middle constraint fails, (7) the upper and lower constraints fail, and (8) the lower constraint fails. The results are as follows.

4.1. All constraints have not failed

It can be seen from Figure4 that under the condition of full restraint without failure, the maximum stress of the crude oil machine support is located at the X-type support frame, where the stress is $7.6975e^5$ Pa, while the stress at the bottom of the support is 13745Pa. The stress at the bottom of the support is far less than that of the X-type support frame. Combined with the yield stress diagram in Figure 5, it can be seen that the yield stress at the joint between the bottom of the bracket and the crude oil machine rotor cover plate is $1.3129e^5$ Pa. This shows that under the condition of full restraint, the stress at the bottom of the support is much lower than its yield stress, and no fatigue failure will occur. At this time, the support can be safely used and play its role in stabilizing the governor of the crude oil machine.

ISSN: 2664-9640

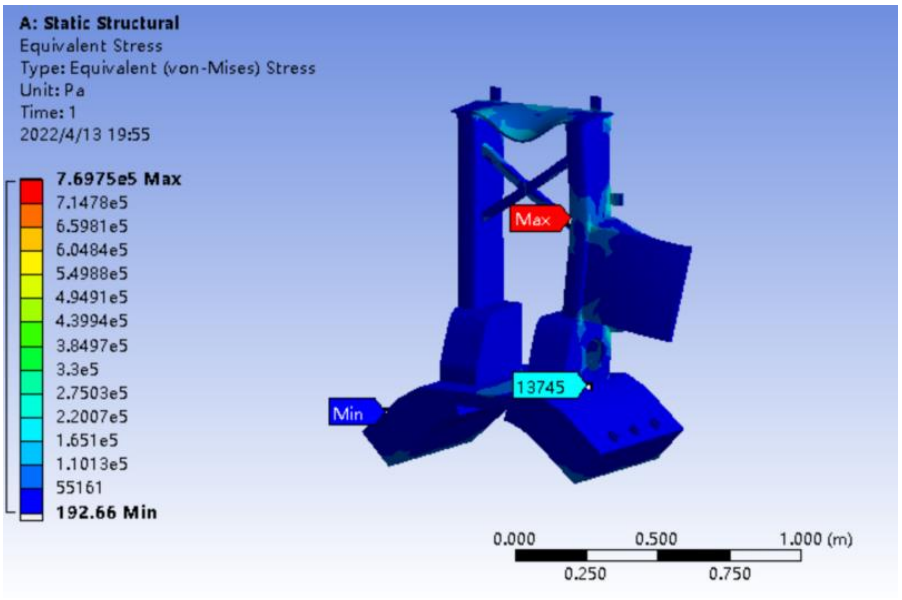

Figure 4: Stress distribution of fully constrained unfailed support

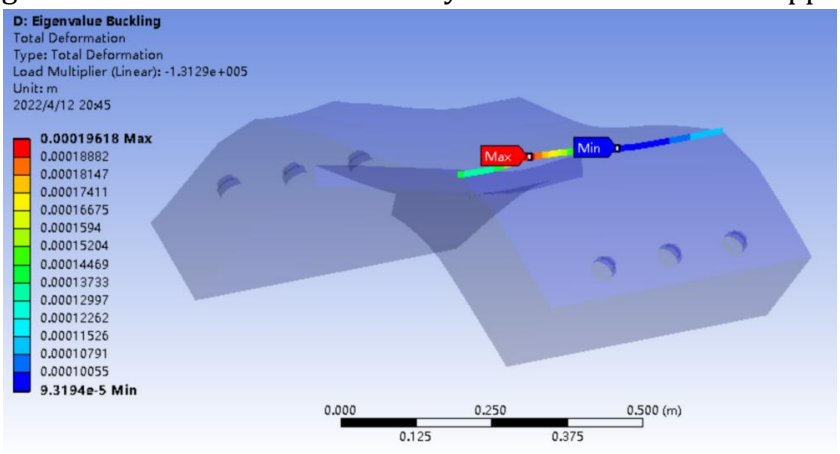

Figure5: Buckling factor of fully constrained and unfailed support joint

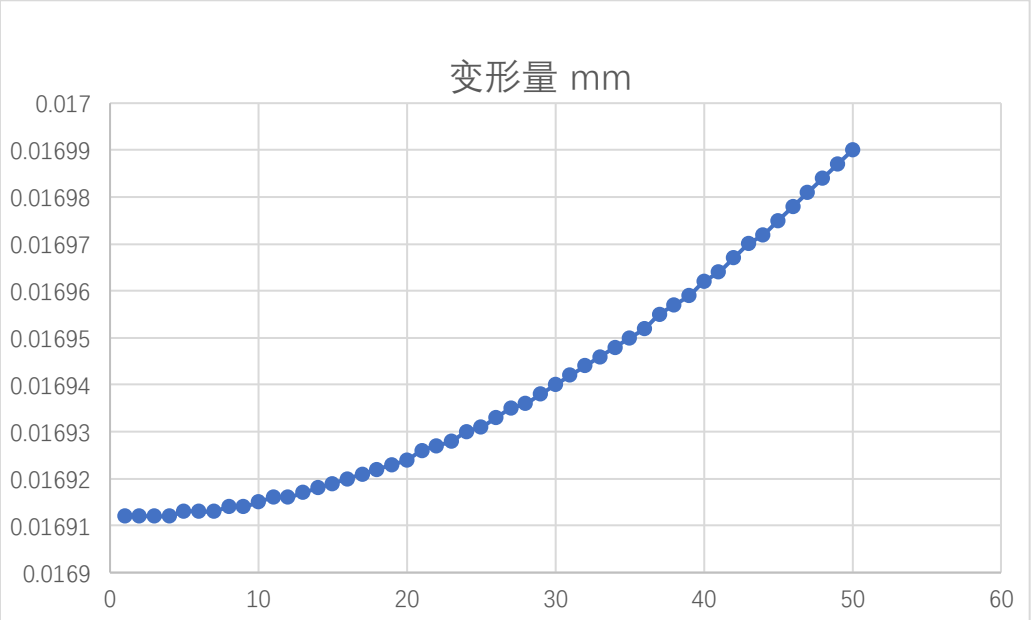

Figure 6: The relationship between the frequency and the deformation of the fully constrained unfailed support

ISSN: 2664-9640

Figure6 shows the relationship between the frequency and the deformation of the support under the action of sinusoidal load under full constraint. With the increase of frequency, the deformation at the bottom of the support gradually rises. The frequency of the crude oil generator is 50Hz, so the maximum deformation under full constraint is 0.008525mm.

4.2. Failure of all constraints

Figure 7 shows the stress distribution of each part of the crude oil support under full constraint failure. It can be seen from the figure that although the maximum stress position is still at the X-type support, the stress at the connection between the bottom of the support and the cover plate of the crude oil support has reached 1.6919e^{5}pa. As can be seen from Figure 8, In the case of full constraint failure, the maximum buckling factor of the bottom joint position is 22695, which is much smaller than the buckling factor generated by the full constraint. The smaller the buckling factor is, the smaller the force required to achieve instability under the same working condition, and the easier it is to enter the unstable state, which will inevitably lead to fracture.

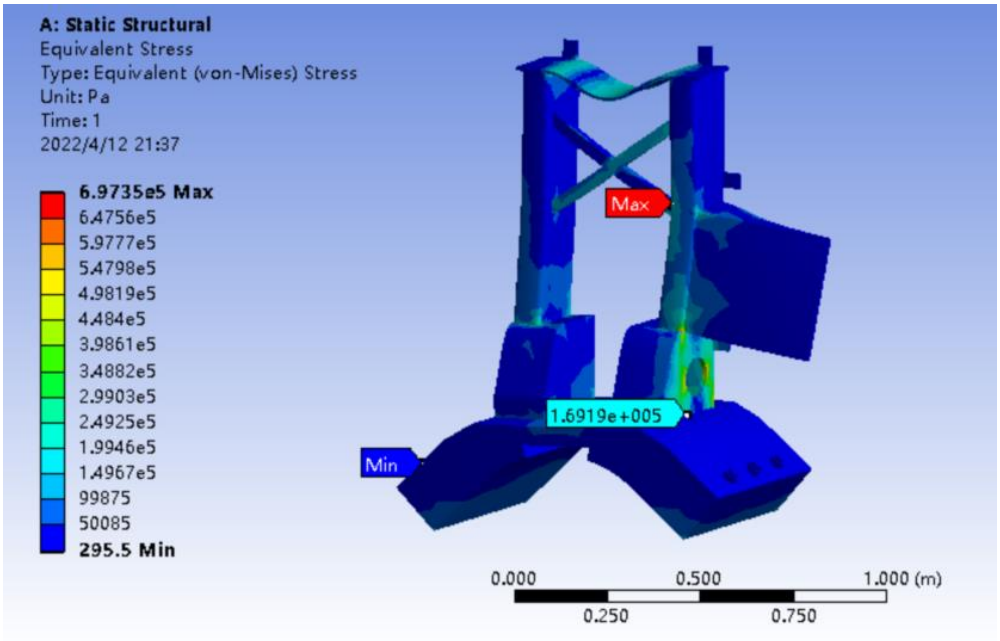

Figure 7: Stress distribution of support under full constraint failure

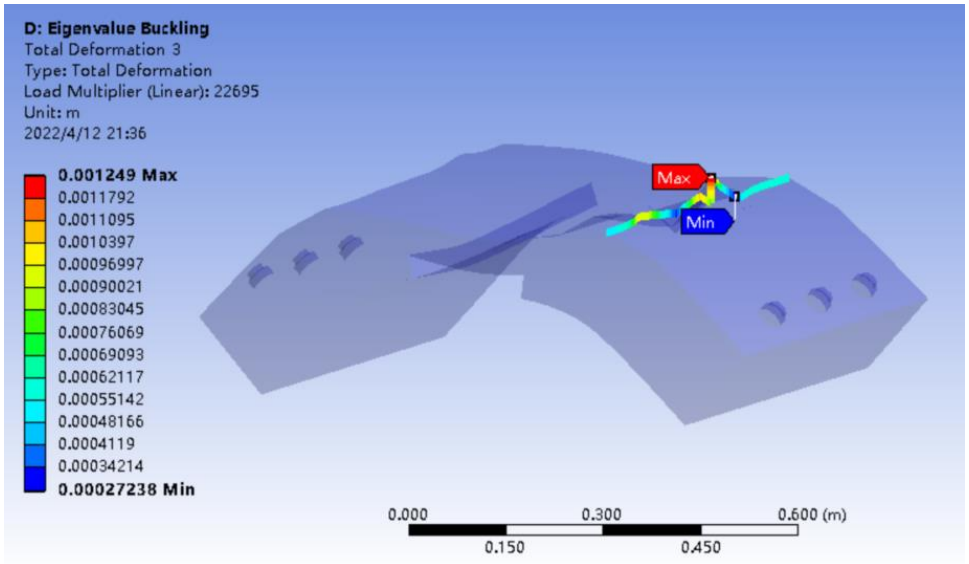

Figure 8: Buckling factor of bracket joint under full constraint failure

ISSN: 2664-9640

Figure9 shows the relationship between frequency and deformation under full constraint failure. It can be seen from Figure9 that the maximum deformation under 50Hz sinusoidal excitation is 0.084421mm, much larger than 0.01699mm under full constraint.

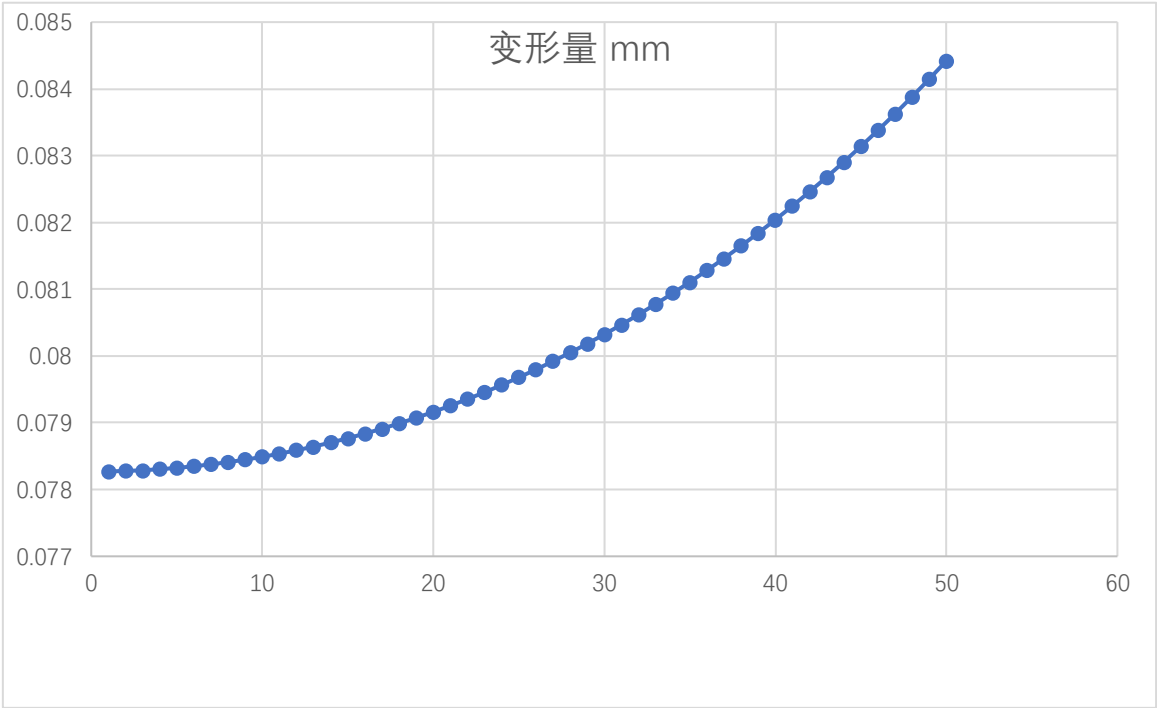

Figure 9: Relationship between the frequency and deformation of the fully constrained failure bracket

4.3. Single constraint failure

Single constraint failure can be divided into three types: upper constraint failure, middle constraint failure and lower constraint failure. Let's take a look at Figure10, which shows the overall statics analysis of crude oil engine support under three single constraint failures: upper, middle and lower. It can be seen from the figure that the maximum stress after the failure of the three constraints is still on the X-shaped support frame, but the upper, middle and lower single constraint failures of the three constraints are $8.4751e^5$ Pa, $8.497e^5$ Pa and $7.768e^5$ Pa respectively, which increase first and then decrease. This is because the design layout of the X-type support frame of the crude oil machine support is relatively close to the upper and middle constraint. When the upper and middle constraint fails, the X-type support frame needs to bear greater mechanical cyclic stress, so its value increases gradually in the finite element analysis cloud diagram, and is larger than the stress under the full constraint state. And under constraint expires, X brace by stress is reduced, and will reduce the stress to the bottom of the bracket and most of the crude oil transfer machine rotor plate, the crude oil machine bracket to counter a generator to produce mechanical vibration cyclic stress, gradually will be part of the stress distribution to the bottom bracket joint, the figure 10 also shows that in the stress of the joints as the constraint failure point down, The stress values of the three single constraint failures are 17117Pa, 41950Pa and 57887Pa, respectively, showing a trend of gradual increase.

ISSN: 2664-9640

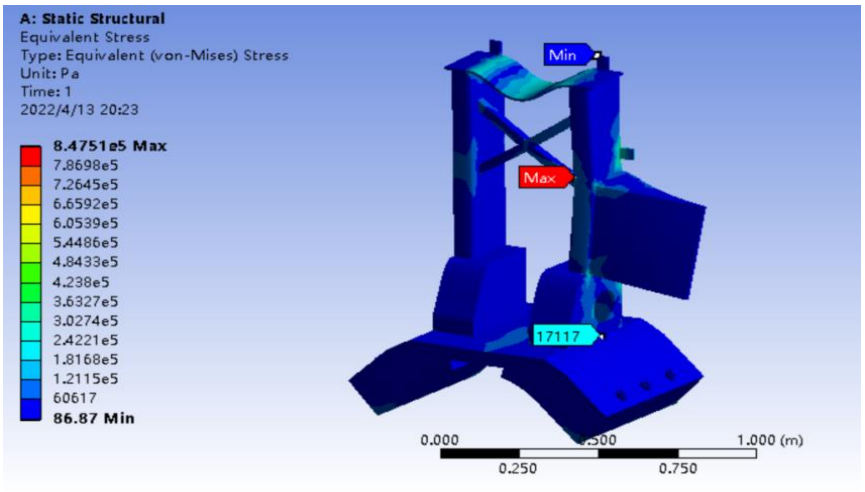

(a)Upper constrained failure stress distribution

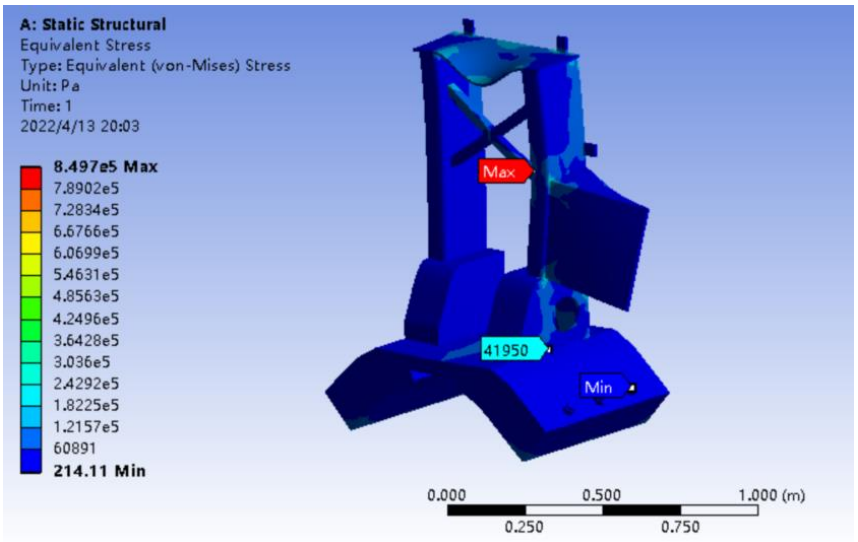

(b) constrained failure stress distribution in

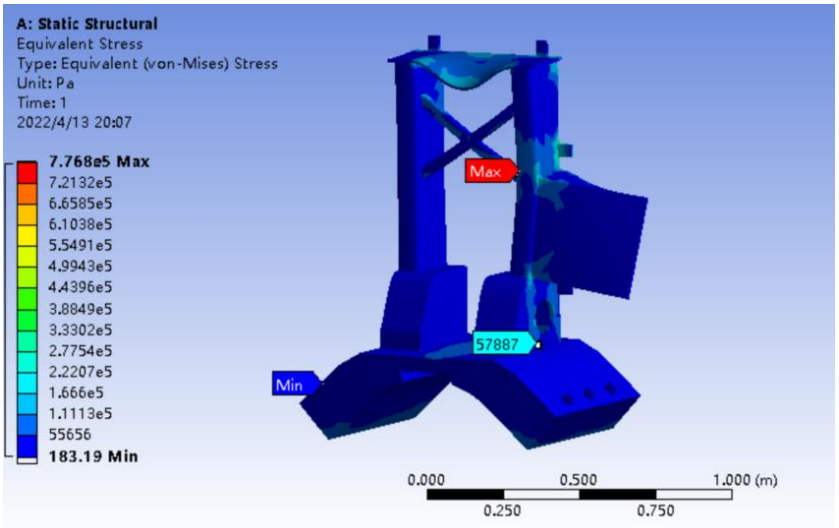

(c)constrained failure stress distribution under

Figure10: Failure stress distribution of three single constraints

Figure11 shows the buckling factor of the joint between the bottom of the support and the base of the crude oil machine under three single constraint failures. It can be seen from Figure11 that the buckling factor of the joint of the support under three single constraint failures is larger than that under the full constraint failure, especially the buckling factor under the medium

ISSN: 2664-9640

constraint failure is the largest. Constraints in the failure cases at this time due to the mechanical vibration cycle bracket joint instability is least likely, and the figure shows on, the two kinds of single constraint failure cases, joint deformation points are on the front end of the bottom of the bracket, and the deformation of failure cases the biggest point is located in the bracket at the bottom of the back-end.

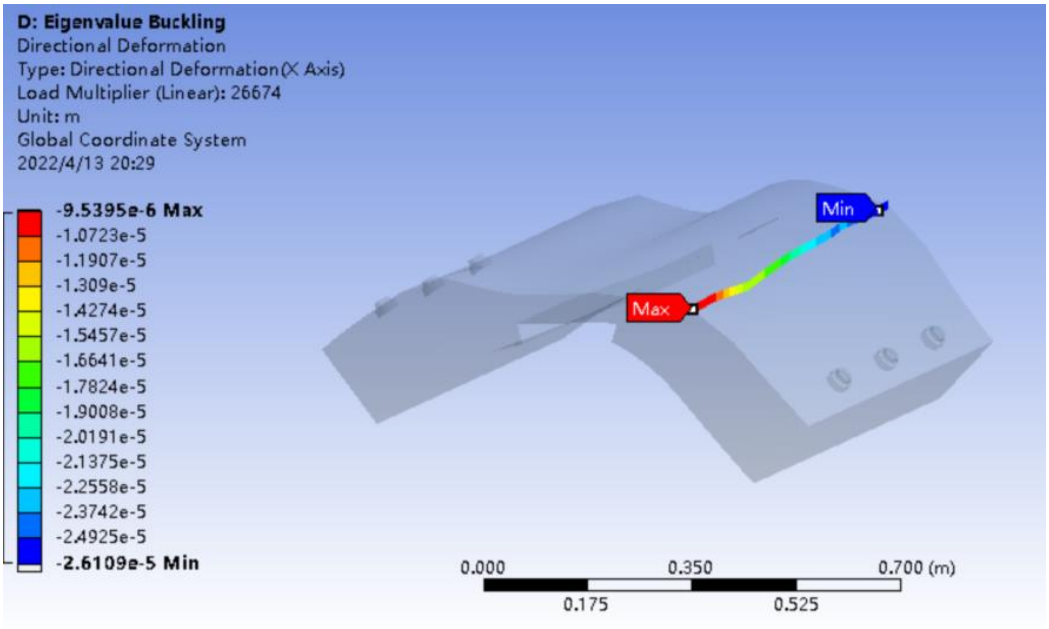

(a)Yield deformation at the bottom joint of the upper constraint failure bracket

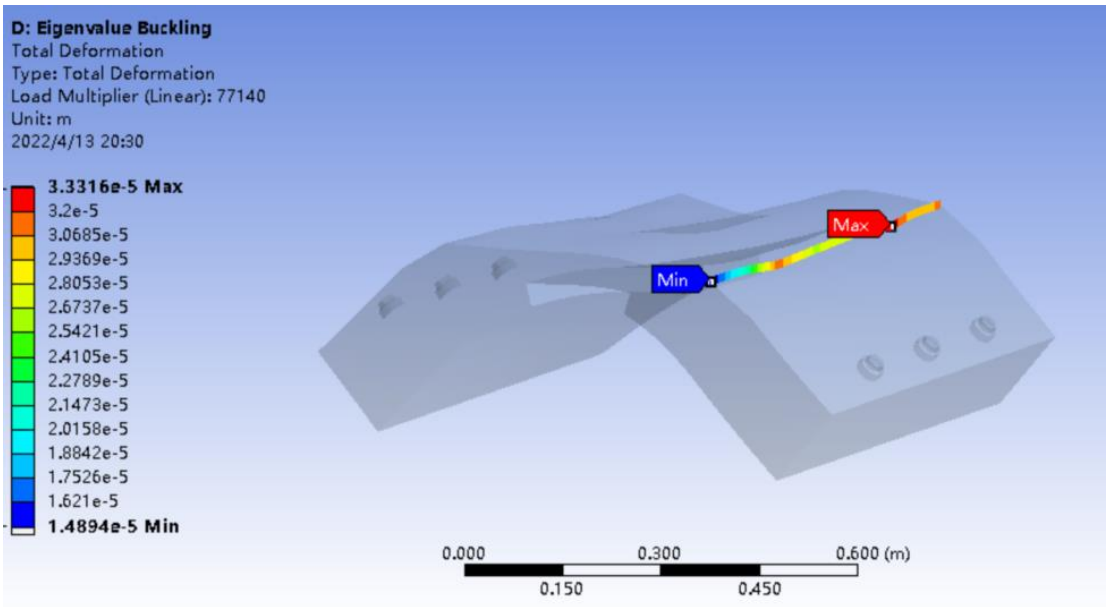

(b)Yield deformation at the bottom joint of the constrained failure bracket in

ISSN: 2664-9640

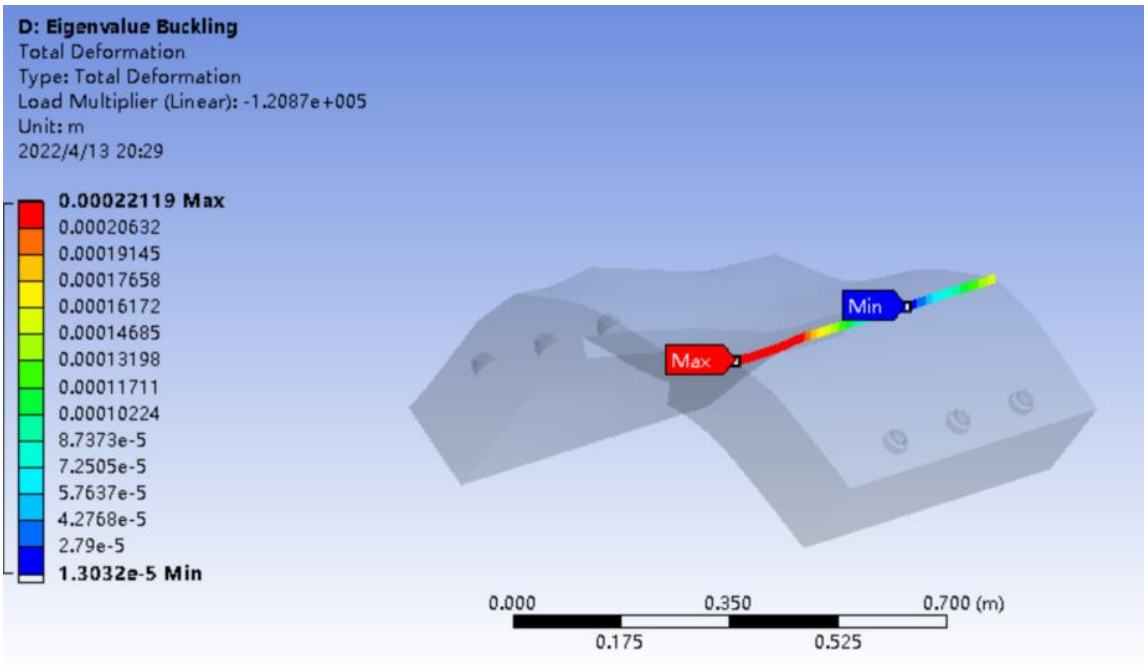

(c)The bottom joint of the lower constraint failure bracket yields deformation

Figure11: Yield deformation at the bottom joint of three single constraint failure supports

Above analysis shows that under the case of single constraint, crude oil machine bracket will not happen by mechanical cycle vibration fatigue fracture, at the same time under the condition of the constraint on the failure of support at the bottom of the stress to a minimum, and the constraint failure cases of buckling failure cases is one of the biggest factors for three, second to failure under constraint conditions, this means that if in production constraints bolt fall off, It can delay the maintenance schedule and will not have a great impact on the support capacity of the crude oil generator bracket.

Figure 12 for three kinds of single failure deformation under different frequency excitation of constraints, the result of the figure 12 (a) (b) (c) three single deformation constraint conditions are presented parabola type increases gradually, while the figure 12 shows the constraints in (d) the failure of the deformation is much larger than the other two, and constraints on the failure and failure deformation of constraints in both difference is not big. At the frequency of 50Hz, the deformation of the lower constraint failure is 0.033843mm, but the deformation is still much smaller than that of the full constraint failure.

4.4. Failure of double constraints

Double constraint failure is divided into upper and middle constraint failure, upper and lower constraint failure and middle and lower constraint failure. Figure 13 for the constraint failure cases of stent stress distribution, the diagram shows the high failure under the condition of constraints, stents as down gradually transferred to the maximum of the leg position, X stand by stress greatly reduced, lost as the function of the vibration of supporting frame, and most of the vibration-proof mainly supported by the support legs. The fluctuation and the failure of the middle and lower constraint comparison can be found that while both the biggest stress points are still in the X type support frame, but the fluctuation of failure cases of constraint X brace than lower constraint failure cases of X brace to withstand greater stress, and stress of the upper and lower constraint at the bottom of the failure of the bracket joint is lower than the middle and lower constraint.

ISSN: 2664-9640

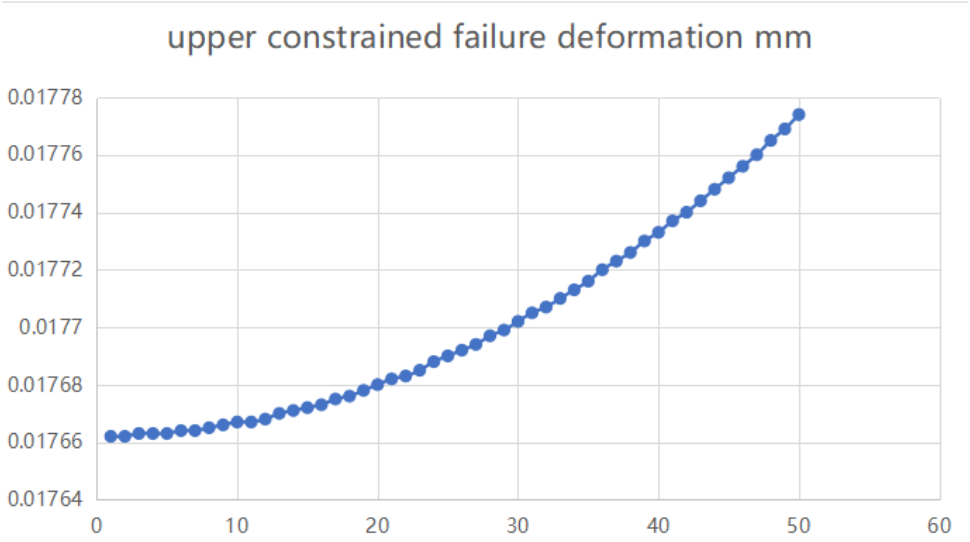

(a)upper constrained failure deformation

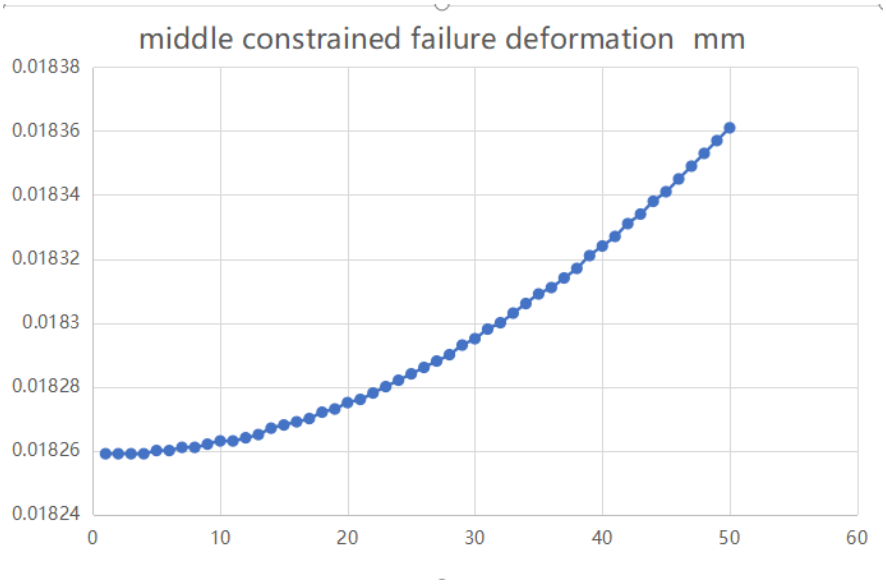

(b)middle constrained failure deformation

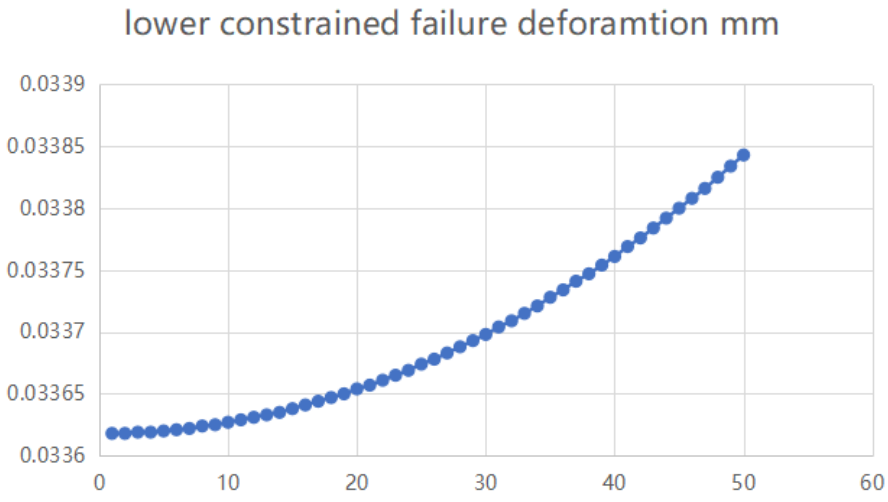

(c) Lower constraint failure deformation

ISSN: 2664-9640

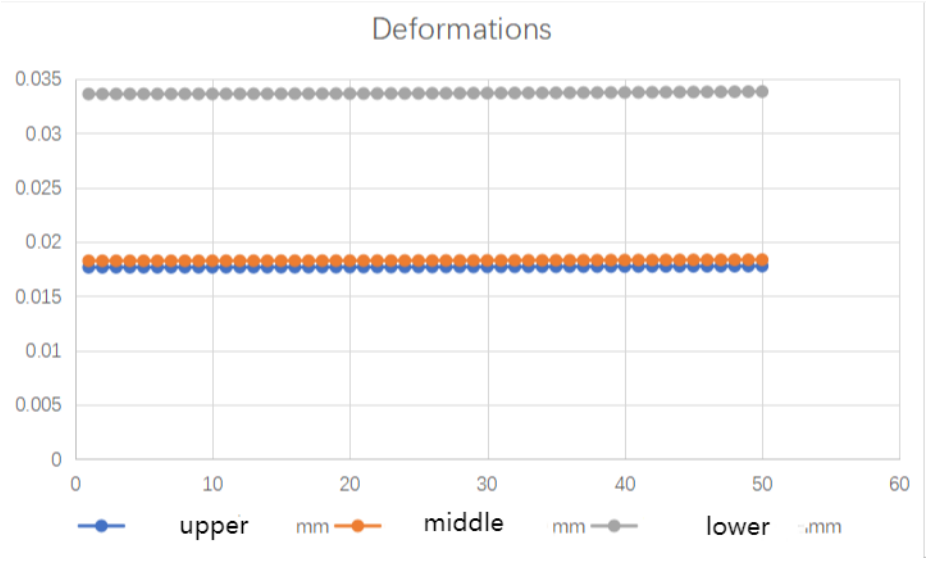

(d) Comparison diagram of three deformations without constraint failure

Figure12: Three deformations with constrained failure

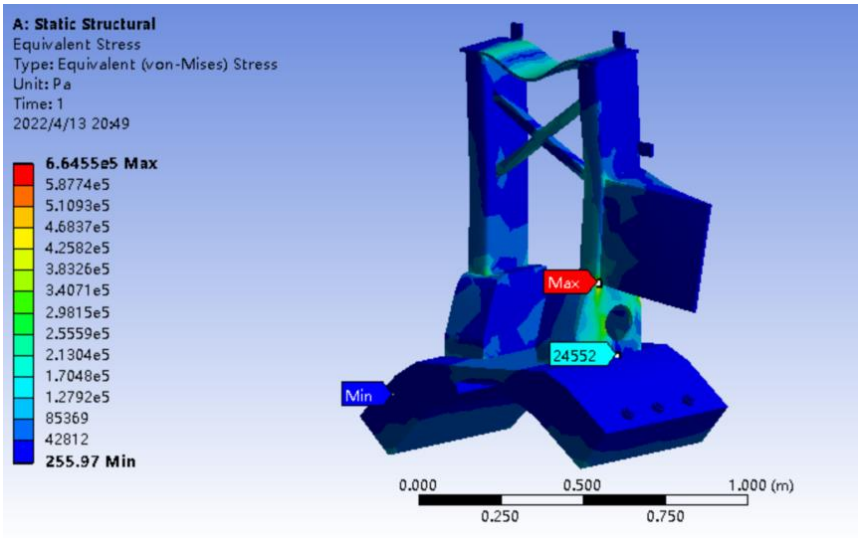

(a)Upper middle constrained failure stress distribution

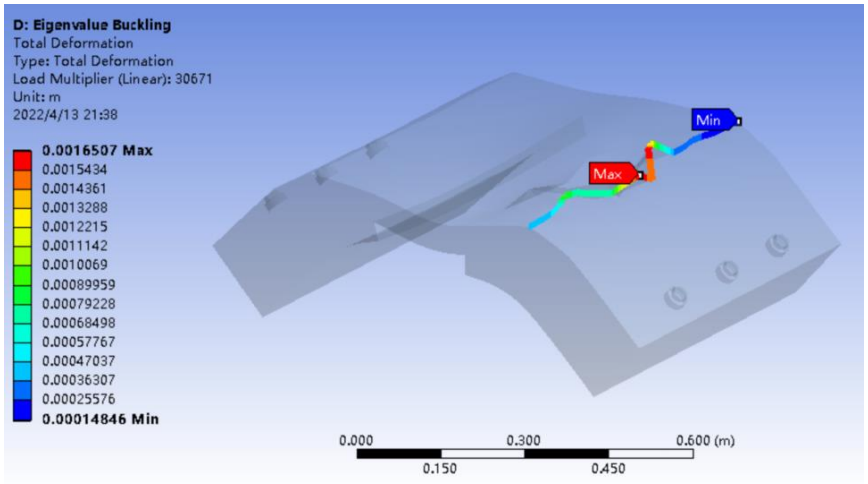

(b) Upper and lower constrained failure stress distribution

ISSN: 2664-9640

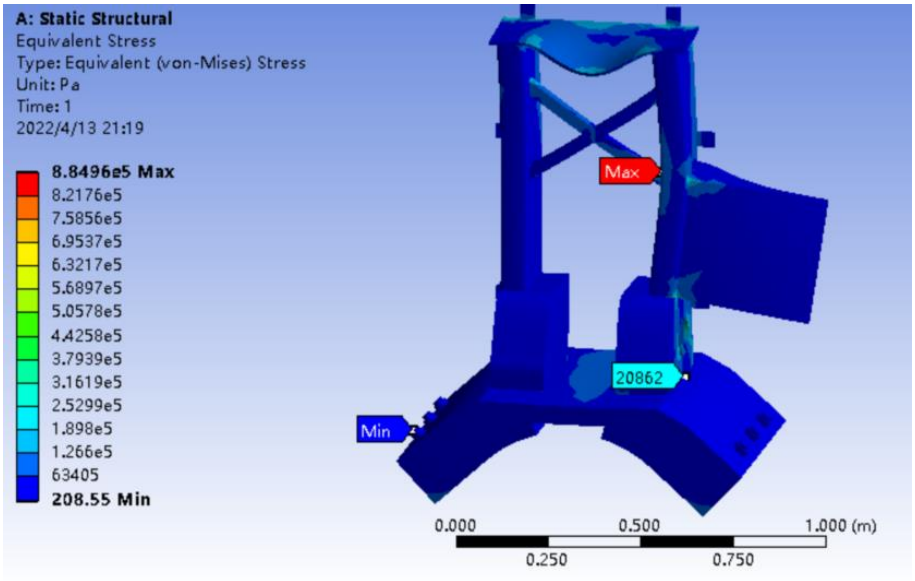

(c) lower constrained failure stress distribution

Figure13: Stress distribution under three double-constraint failure conditions

As can be seen from Figure 13, the stresses at the bottom joints of the support under three double-constraint failures are respectively 30671Pa, 24562Pa and 61224Pa. By comparing them with the three constraint failures in Figure 11, it can be seen that the stress of the crude oil machine support under single constraint failure is smaller than that under double constraint failure.

Figure14 shows that the maximum buckling factor under double constraint failure is 61224, while the minimum buckling factor is 24562. At this time, the buckling factor under upper and lower constraint failure has begun to approach the buckling factor under full constraint failure.

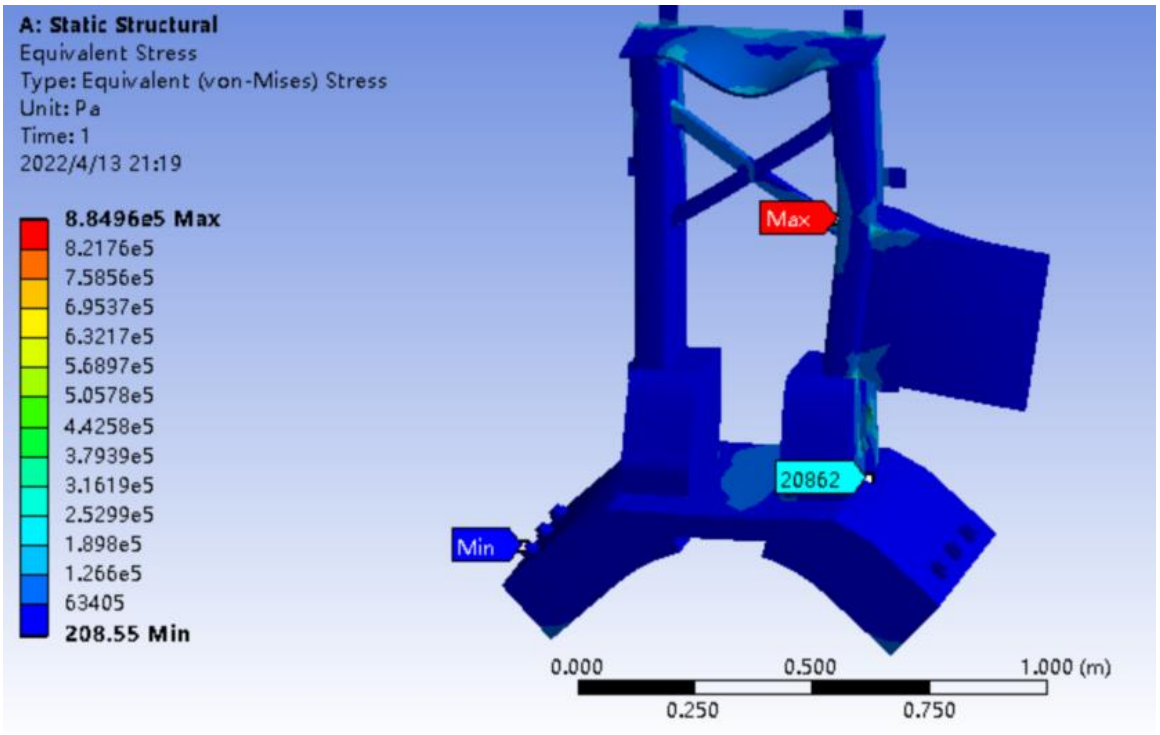

(a)Buckling deformation at the bottom joint of the upper middle constraint failure support

ISSN: 2664-9640

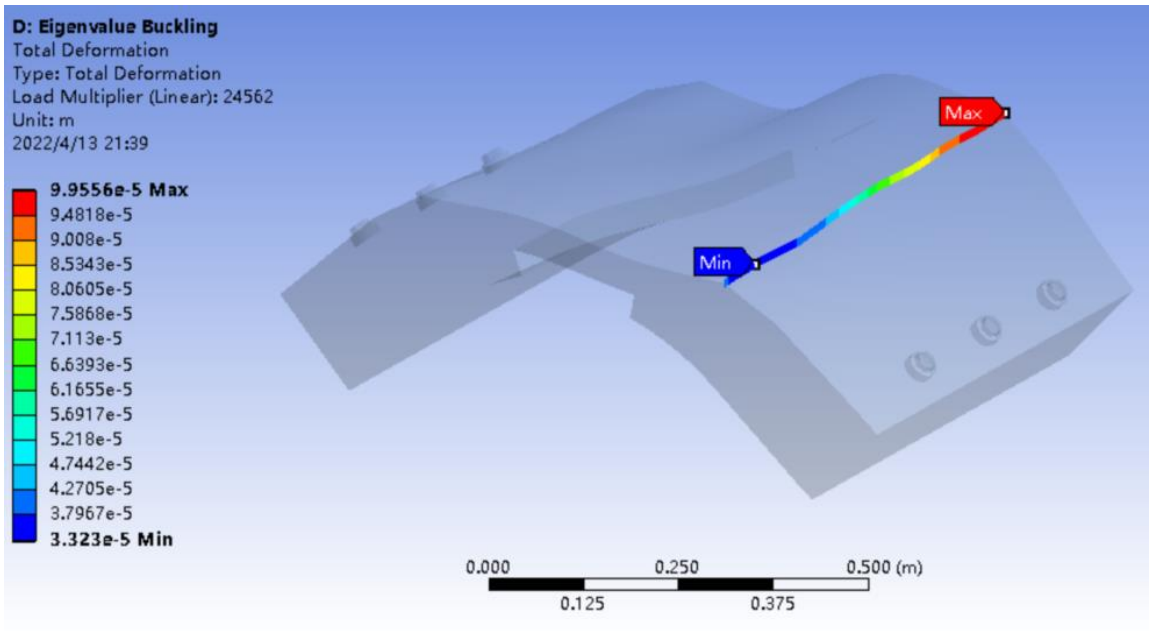

(b)Buckling deformation at the bottom joint of the upper and lower constraint failure support

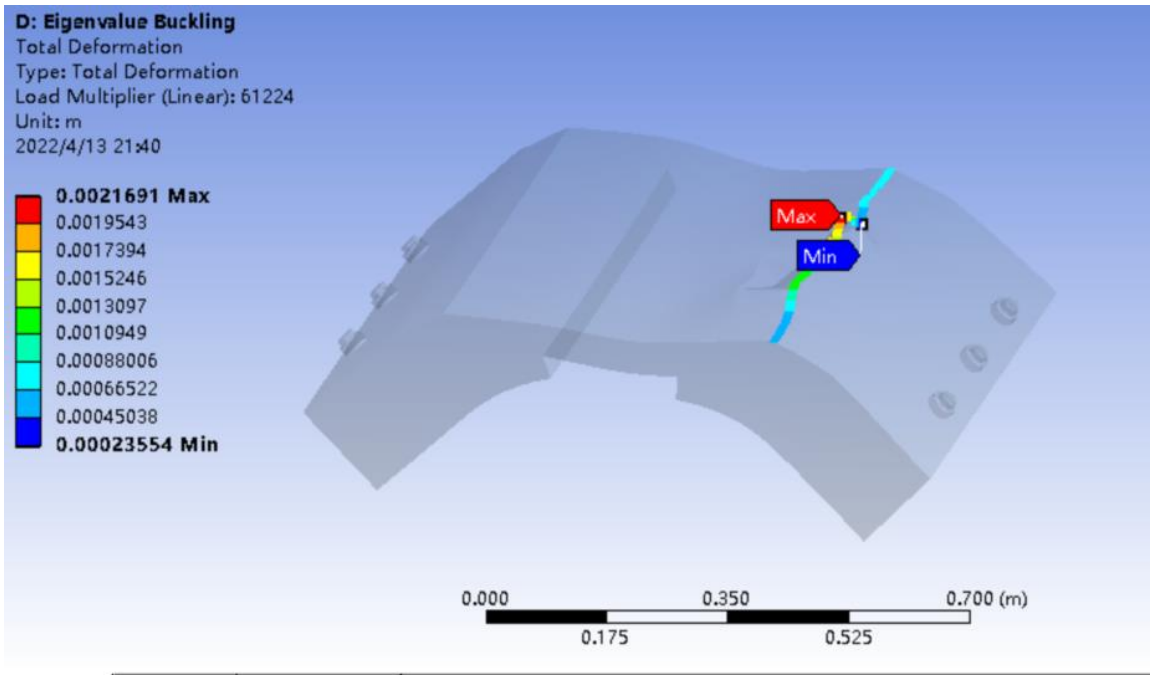

(c) Buckling deformation at the bottom joint of the middle and lower constraint failure support

Figure14: Buckling deformation at the bottom joint of three types of double constraint failure supports

Figure15 shows the relationship between the frequency and the deformation of the support under double constraint failure. It can be seen from the figure that the deformation of the support under three constraint failure conditions gradually rises in a parabolic manner with the increase of frequency. The minimum deformation of the upper and middle constraint failure is 0.026267mm at 50Hz, and the maximum deformation of the middle and lower constraint failure is 0.043279mm. By comparing Figure15 (d) and Figure13 (d), it can be seen that the gap between the three deformations in the case of double constraint failure is not as big as that between the three deformations in the case of single constraint failure. The maximum deformation of 0.026266mm under the failure of upper and middle constraints is smaller than

ISSN: 2664-9640

0.033843mm under the failure of lower constraints, indicating that the influence of lower constraints on the stress of the support is greater than that of the other two constraints.

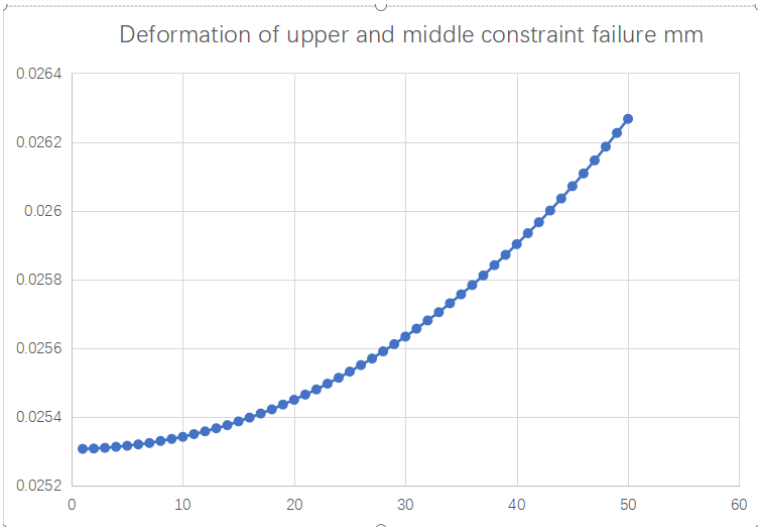

(a)Deformation of upper and middle constraint failure

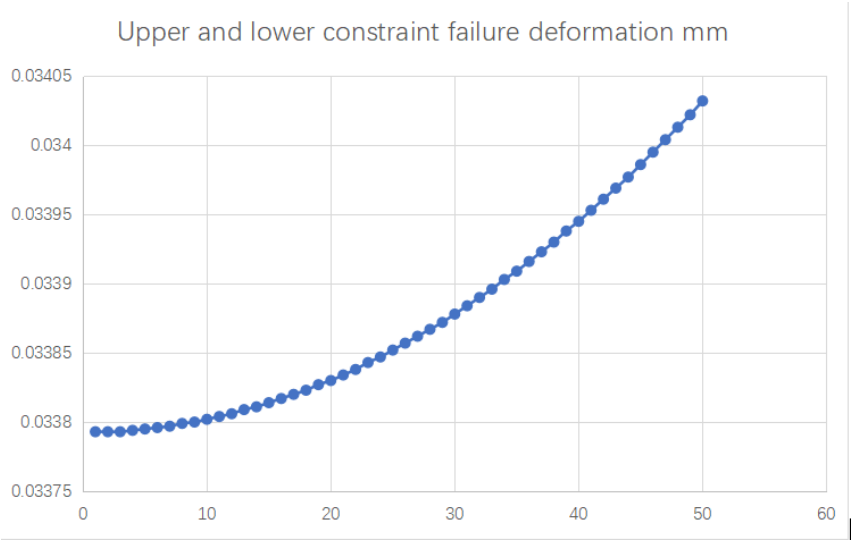

(b)Upper and lower constraint failure deformation

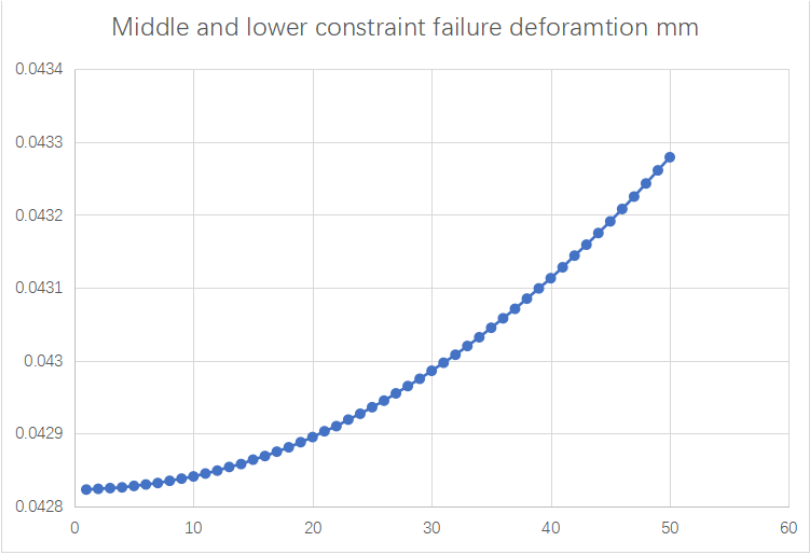

(c)Middle and lower constraint failure deformation

ISSN: 2664-9640

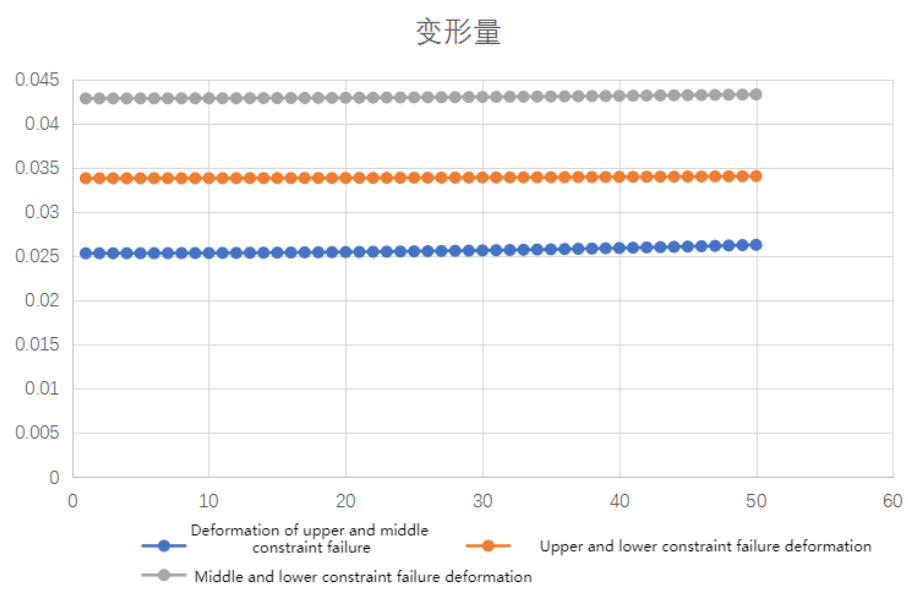

(d)Comparison diagram of deformation of three kinds of double constraint failure

Figure15: Three different deformations of double constraint failure

5. Failure cause solution

Based on the result of the failure cause analysis, known in all the constraints not failure, single or double constraints bracket joint failure, all constraint conditions of stress and deformation and suffered the change of the buckling factor, including all constraints failure cases bracket joint stress, maximum deformation, the largest buckling factor to the minimum, Therefore, in this section, the optimal design of reinforcement is mainly carried out under the condition of full constraint failure to improve the strength of the bracket connection. The three-dimensional numerical model is shown in Figure16.

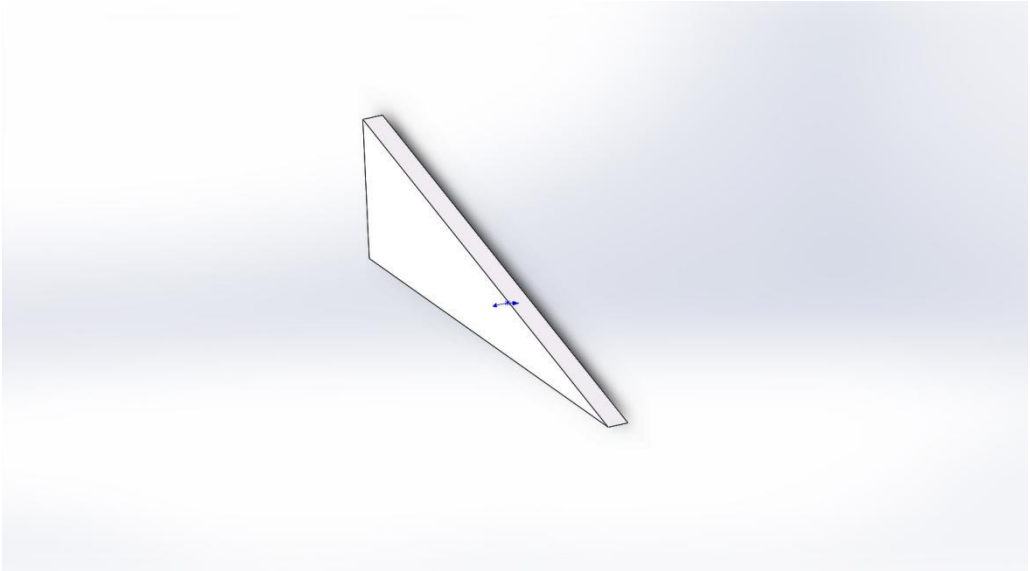

Figure 16: Stiffener

There are three design parameters of the stiffeners, namely height, bottom length and thickness. This paper will design the stiffeners from these three aspects to ensure that the support can still maintain the stability of the support under the condition of full constraint failure.

ISSN: 2664-9640

5.1. The influence of reinforcement thickness on the stress at the joint of the bracket

According to the original size of the crude oil machine support, the height, length and thickness of the reinforcement are limited, and the height selection range is between 20mm and 80mm; Length selection range is 20mm to 92.4mm; The thickness is selected from 1mm to 50mm. The height is 10mm, the length is 92.4mm, and the thickness is set to be between 1mm and 50mm for calculation. Figure17 is the comparison diagram of deformation at the joints of brackets with different thicknesses after calculation.

It can be seen from Figure17 that the deformation of the bracket gradually decreases with the increase of thickness, and the deformation at the joint of the bracket changes the most in the interval from 1mm to 30mm, while the deformation decreases in the interval from 30mm to 50mm, but the decrease is small. When the thickness of the stiffener is minimum 1 mm, the bracket joint deformation is only 0.015154418 mm, with the Figure 12 and 15 (a) the minimum deformation in contrast, its value than failure deformation of a single failure and dual constraints of the minimum value is smaller, shows that after adding reinforced bracket joint deformation has obvious decrease, And it gradually decreases with the increase of the thickness of reinforcement.

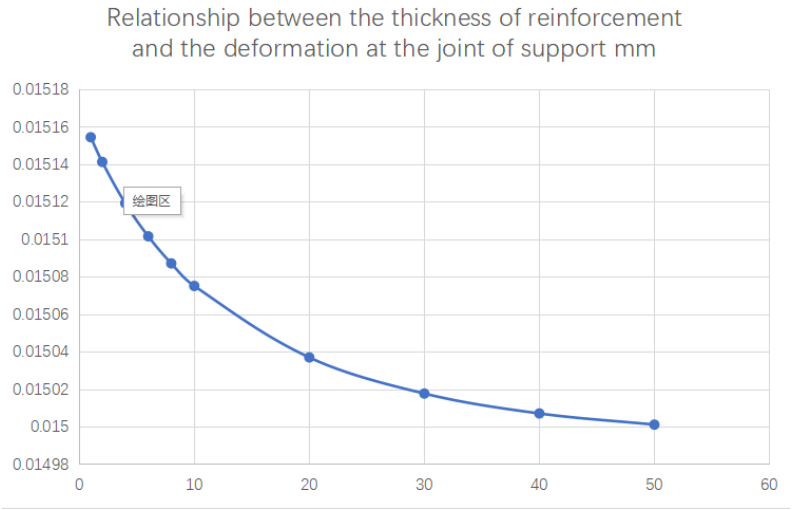

Figure17: Relationship between the thickness of reinforcement and the deformation at the joint of support

Figure18 shows the relationship between the stiffener thickness and the stress on the stiffener at the connection of the bracket. It can be seen from Figure18 (a) that with the increase of the thickness of the reinforcement, the stress at the joint of the support gradually increases. Figure18 (b) shows that with the increase of the thickness of the stiffeners, the stress on the stiffeners gradually decreases. Combined with the comparison of two stresses in Figure18 (c), it can be seen that the variation of the stress on the stiffeners under the same increase of the thickness of the stiffeners is much larger than the stress at the joint of the supports. Combined with Figure17, it can be seen that the thickness between 30mm and 40mm should be selected when selecting the thickness of the reinforcement. At this time, the thickness can obtain the maximum stress of the reinforcement and the minimum deformation at the connection of the support as far as possible under the condition that the stress at the connection of the support is small.

ISSN: 2664-9640

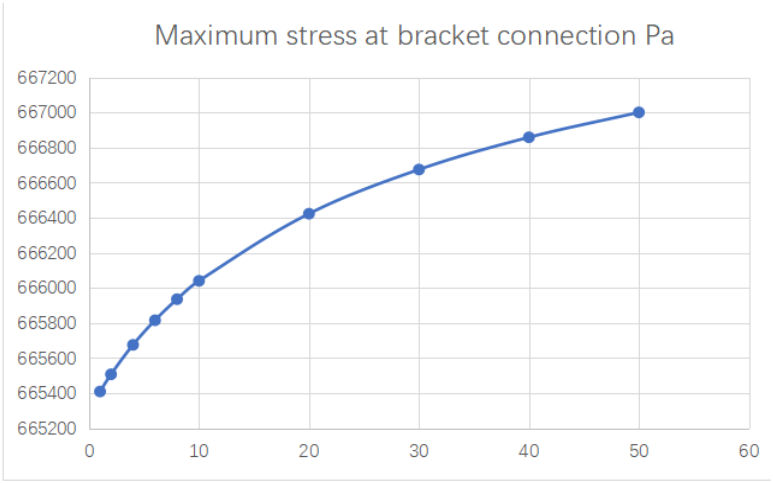

(a)The relationship between the thickness of stiffeners and the stress of fully constrained failure scaffolds

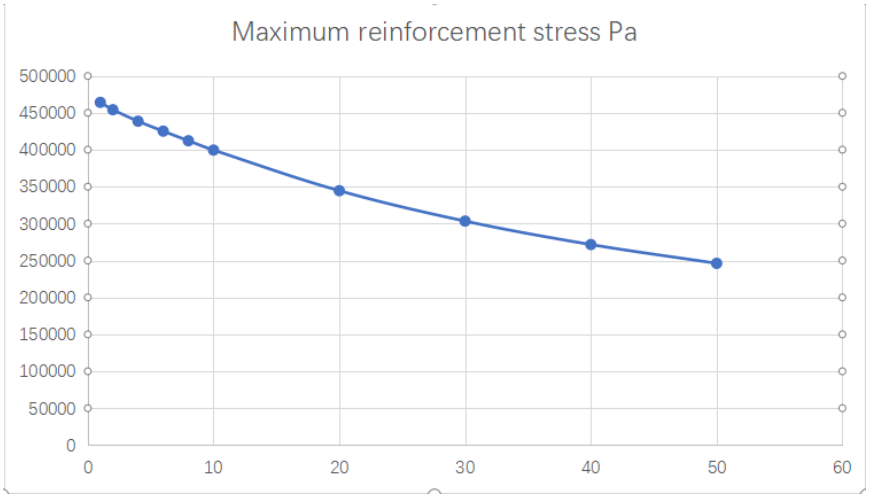

(b)The relationship between stiffener thickness and stiffener stress of fully constrained failure brackets

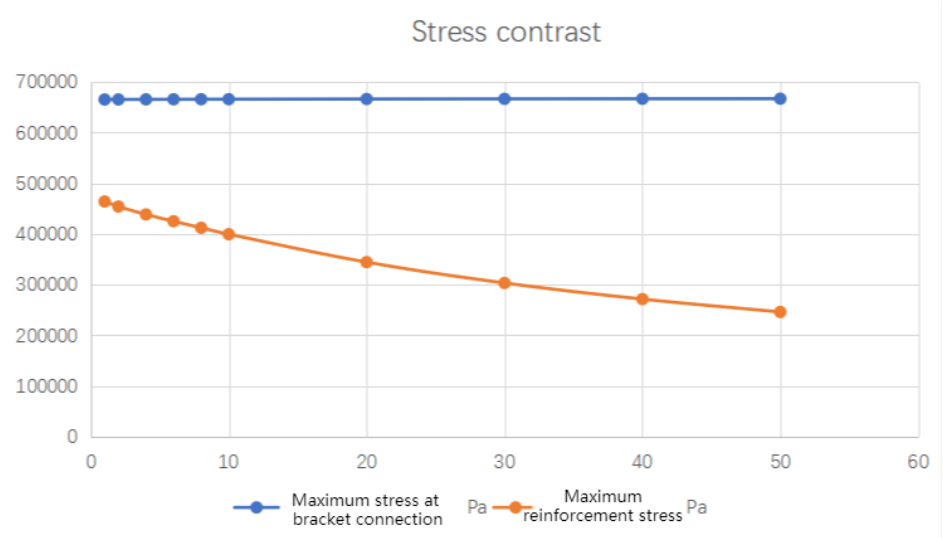

(c) The relationship between reinforcement stress and stent stress of fully constrained failure scaffolds

Figure18: Influence of stiffener thickness on support

ISSN: 2664-9640

5.2. The influence of reinforcement height on the stress at the joint of the bracket

According to the control variable method and the actual size of the field, the height of the reinforcement is selected as 20mm to 80mm, the length is 92.4mm to 20mm, and the thickness is still selected as 1mm to 50mm for static stress analysis under cyclic mechanical load.

Figure 19 shows the influence of reinforcement structures of different heights on the stress of the crude oil machine support in the interval from 20mm to 80mm. It can be seen from the figure that with the increase of reinforcement thickness, the stress of the support gradually rises, but the increase amplitude is very small. Among them, the stress of the 80mm height reinforcement is the largest, but there is little difference between it and other height reinforcement.

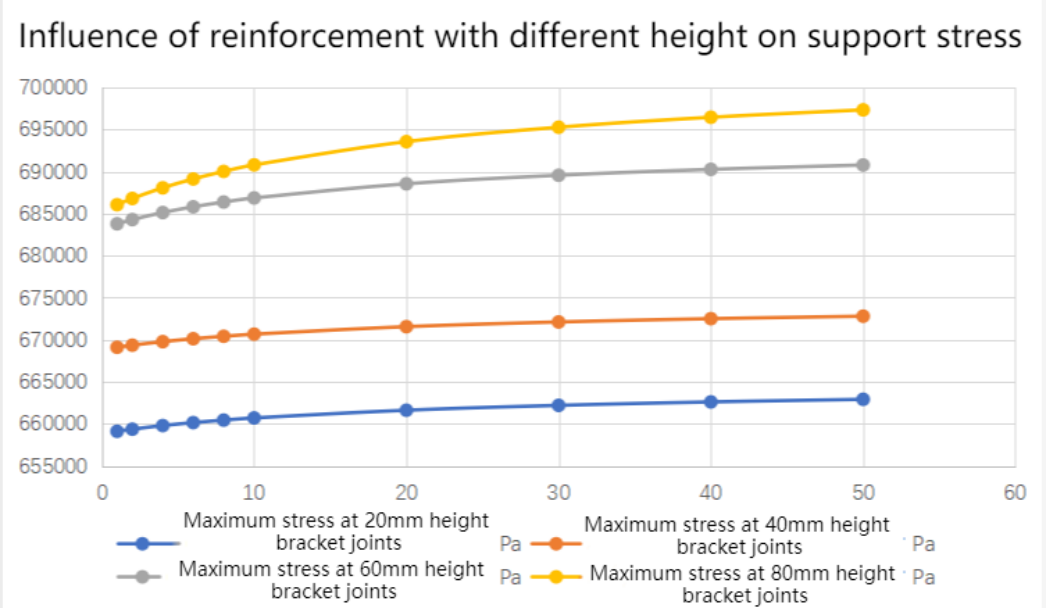

Figure19: Influence of reinforcement with different height on support stress

Figure20 shows the comparison of the stresses of reinforcement bars with different heights. It can be seen that the stress of reinforcement bars decreases gradually with the increase of thickness, and the stress of reinforcement bars with a height of 60mm is the least. In the thickness range of 1mm to 20mm, the stress of 20mm height reinforcement is less than that of 40mm height reinforcement. However, when the thickness of reinforcement is greater than 20mm, the stress of 20mm height reinforcement is gradually greater than that of 40mm height reinforcement. By comparing with Figure 19, it can be seen that the influence of the increase of the height and thickness of the stiffeners on the stress of the stiffeners is greater than the influence of the stress at the connection of the supports, which means that the stress analysis of the stiffeners should be given priority to in the actual design and analysis.

Figure 21 shows the influence of reinforcement with different heights on the deformation at the joint of the bracket. It can be seen from FIG. 22 that when the thickness of reinforcement is in the range of 1mm to 5mm, the minimum deformation of reinforcement is in the range of 40mm; however, when the thickness rises from 5mm to 10mm, the minimum deformation of reinforcement is in the range of 80mm. And the deformation of 60mm height reinforcement is also lower than that of 40mm reinforcement.

In the range of 10mm to 20mm reinforcement thickness, the deformation at the joint of the bracket gradually decreases with the increase of thickness, and the minimum deformation at this time is the 80mm height reinforcement. When the thickness of the reinforcement increases gradually from 20mm, the deformation of the 40mm reinforcement height still decreases gradually, but the decrease is very small, while the deformation of the other reinforcement

ISSN: 2664-9640

height increases gradually with the increase of the thickness, and the deformation of the 80mm reinforcement height increases the most.

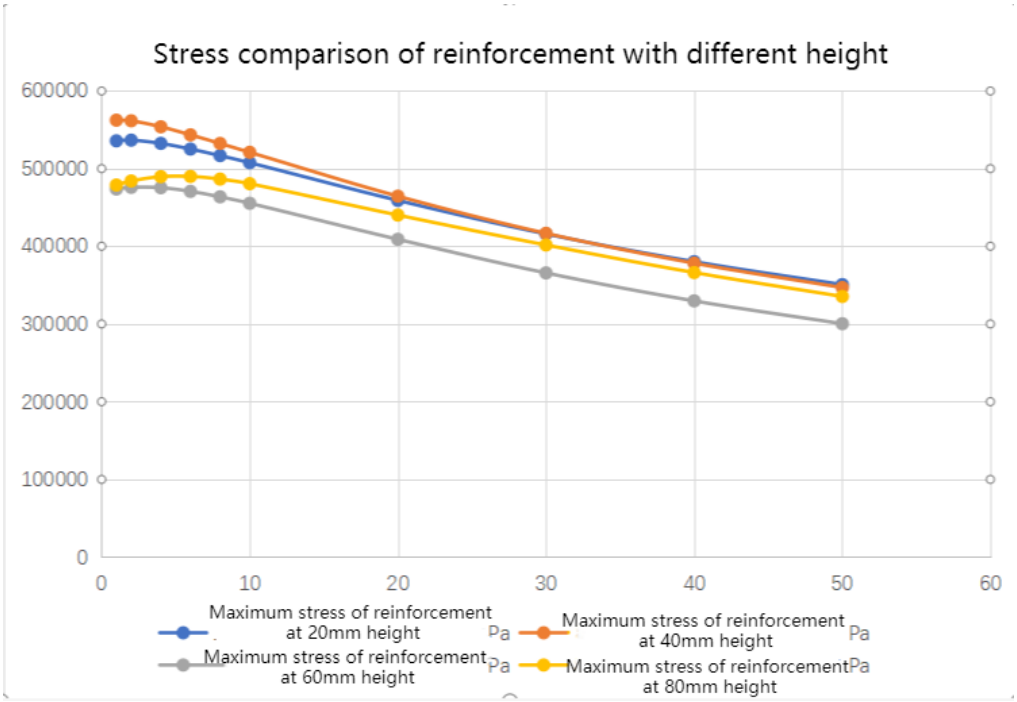

Figure 20: Stress comparison of reinforcement with different height

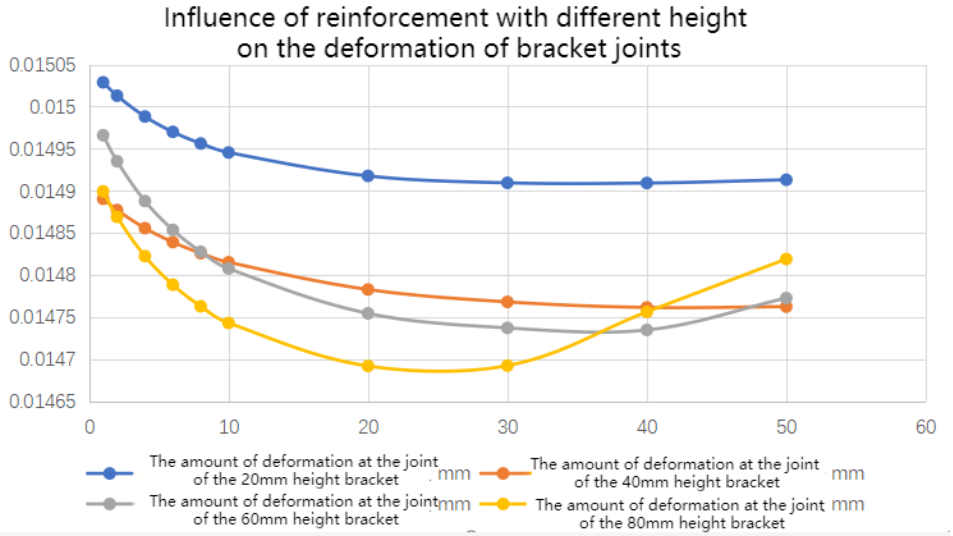

Figure 21: Influence of reinforcement with different height on the deformation of bracket joints

Figure 22 shows the comparison of the buckling factors of the reinforcement bars with different heights. It can be seen from the figure that when the thickness of the reinforcement bars is greater than 8mm, the buckling factors of the reinforcement bars with 20mm to 80mm height are larger than the buckling factors of the fully constrained failure. And the buckling factor of the 20mm and 40mm height reinforcement can exceed the buckling factor of the full restraint failure at the minimum thickness of 4mm reinforcement, while the maximum buckling factor of the thickness range of 10mm to 18mm reinforcement is the height of 60mm reinforcement. The maximum buckling factor after 18mm is located at 80mm height of the stiffeners.

ISSN: 2664-9640

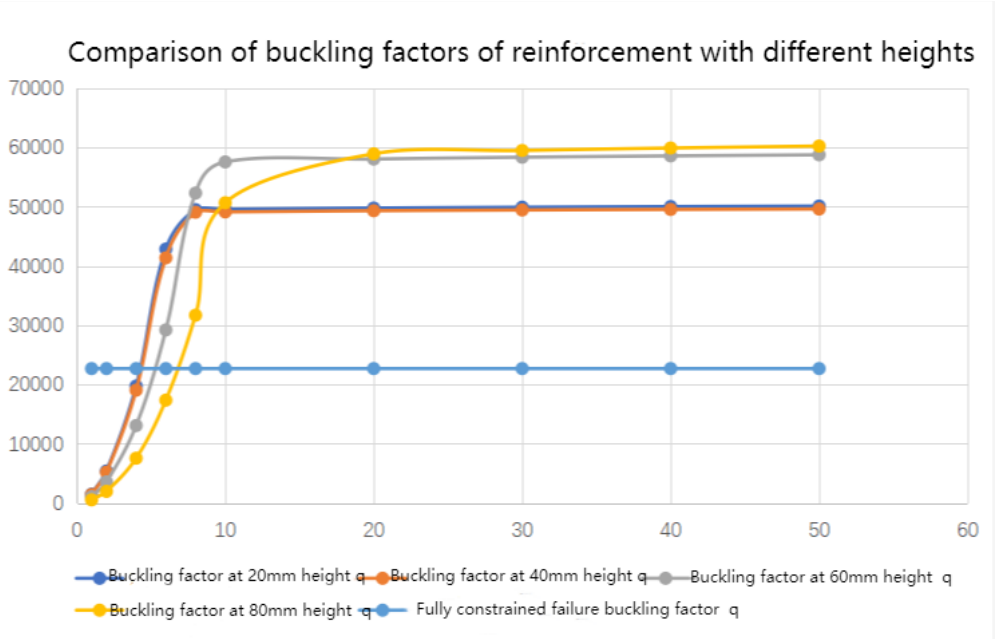

Figure 22: Comparison of buckling factors of reinforcement with different heights

Combined with Figures 19 to 22, it can be seen that when the thickness of the reinforcement is between 20mm and 30mm, the deformation is the smallest. Meanwhile, the maximum buckling factor of the reinforcement in the thickness interval between 20 and 30mm is that of the reinforcement with a height of 80mm, and the stress of the reinforcement with a height of 80mm is only greater than that of the reinforcement with a height of 60mm.

5.3. The effect of reinforcement length on the stress at the joint of the bracket

The length parameters of the reinforcement are in the range of 20mm to 92.4mm, the height is selected to be between 20mm to 80mm, and the thickness is between 1mm to 50mm. Figure23 shows the relationship between the reinforcement with different lengths and the stress of the support, the stress of the reinforcement and the deformation at the connection of the support at 20mm height. Figure23 (a) shows the influence of different lengths of stiffeners on the stress of the support. It can be seen from the figure that when the length of stiffeners is 40mm and 92.4mm, the stress at the connection of the support is the smallest, while when the length of stiffeners is 20mm, 60mm and 80mm, the stress at the connection of the support is not significantly different. Figure23 (b) shows that when the thickness of the reinforcement is within the range of 1mm to 5mm, the length of the reinforcement with minimum deformation at the joint of the bracket is 20mm; when the thickness of the reinforcement is greater than 5mm, the length of the reinforcement with minimum deformation at the joint of the bracket is 92.4mm with the increase of the thickness. Figure23 (c) shows that as the thickness of the reinforcement increases, the overall stress of the reinforcement gradually decreases. Within the thickness range of 1mm to 15mm, the stress of the 20mm thickness reinforcement is the least, but after the thickness exceeds 15mm, the stress of the 80mm height reinforcement is the least. However, the maximum stress of the 92.4mm-long reinforcement is the largest. Combined with Figure23 (a) and (b), it can be seen that when the 92.4mm-long reinforcement is used, the overall stress of the bracket is mainly borne by the reinforcement, so as to avoid excessive stress and fatigue rupture at the joint of the bracket. Figure23 (d) shows that the buckling factors of the stiffeners with different lengths of 20mm after the thickness of the stiffeners is greater than 4mm are all larger than the buckling factors under the condition of full constraint failure, and the maximum buckling factors are located at the stiffeners with 80mm length.

Therefore, when the height is 20mm, the length of the reinforcement is 92.4mm, and the thickness is 40mm to 50mm, the reinforcement is the best working condition.

ISSN: 2664-9640

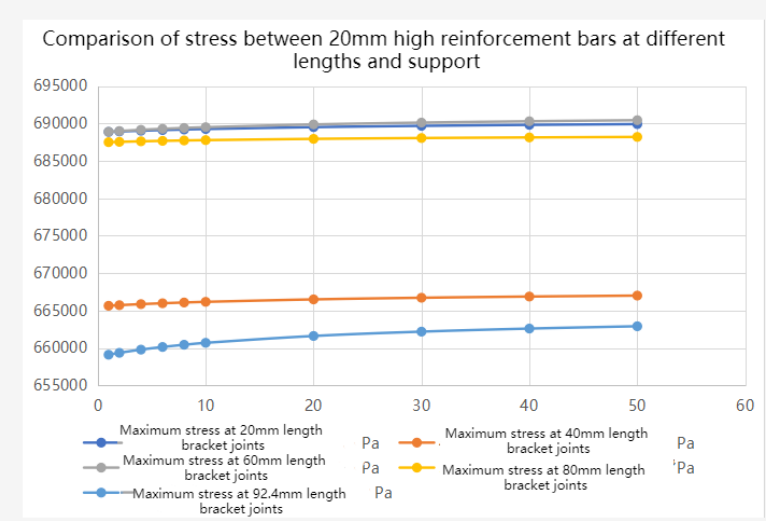

(a) Comparison of stress between 20mm high reinforcement bars at different lengths and support

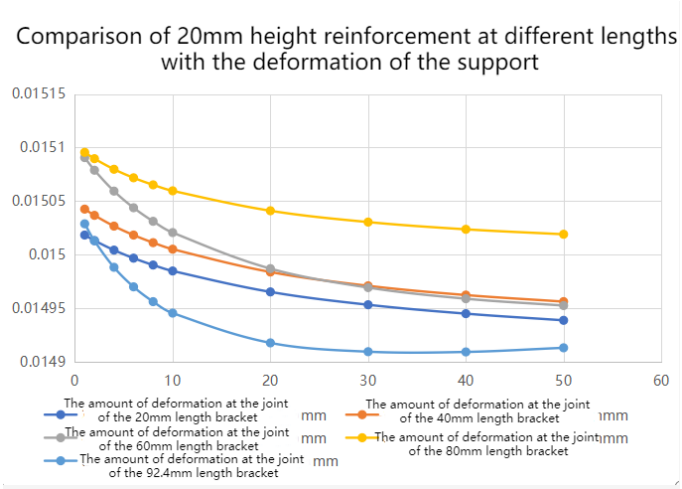

(b) Comparison of 20mm height reinforcement at different lengths with the deformation of the support

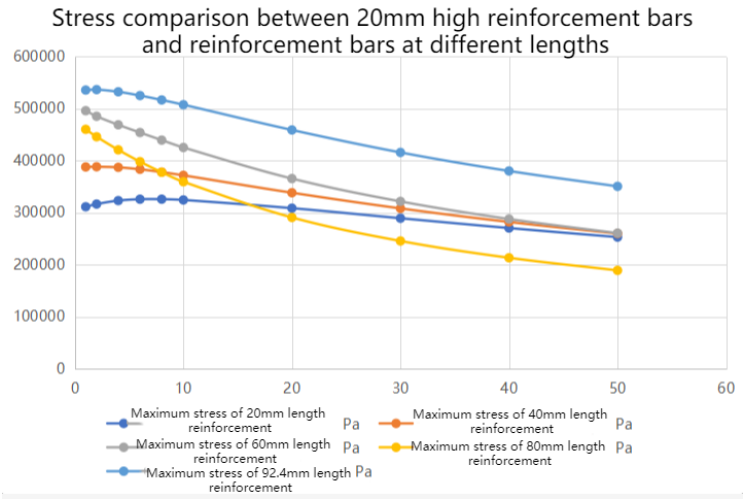

(c)Stress comparison between 20mm high reinforcement bars and reinforcement bars at different lengths

ISSN: 2664-9640

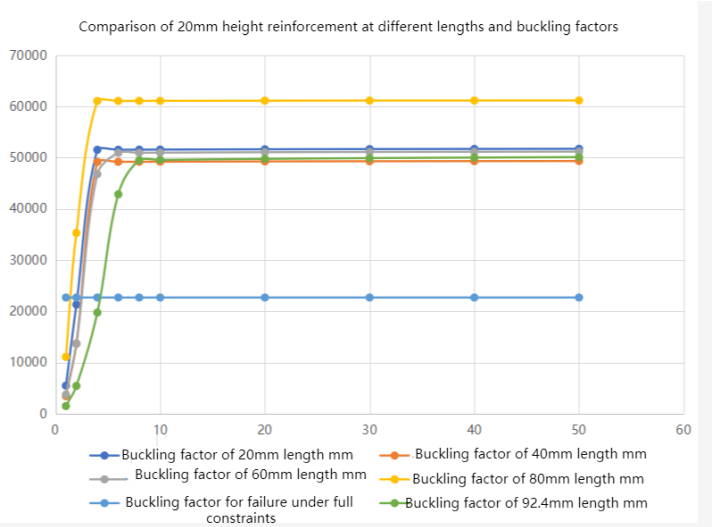

(d) Comparison of 20mm height reinforcement at different lengths and buckling factors

Figure 23: Relationship between different heights of 20mm high reinforcement bars and the support

Figure24 shows the relationship between the 40mm height reinforcement and the stress and deformation of the support in the length range of 20mm to 92.4mm. It can be seen from Figure 24 (a) that the stress of the bracket with 20mm reinforcement length is much greater than that of the bracket with other lengths of reinforcement, so the stress and deformation of the 20mm reinforcement length are too large to be considered. Figure 24 (b) shows the influence of stress on the bracket with 40mm to 92.4mm reinforcement. It can be seen that the bracket with 60mm reinforcement suffers the least stress.

Combined with Figure 24 (c) and (d), it can be seen that the minimum deformation is 92.4mm in length, followed by the deformation at the joint of the bracket with 40mm reinforcement. However, the stress of the 92.4mm length stiffener bracket is much greater than that of the 40mm length stiffener bracket. Combined with Figure24 (E), it can be seen that the maximum buckling factor is located at the 92.4mm length stiffener when the thickness of the stiffener is greater than 8mm, while the buckling factor of the 40mm length stiffener is only less than that of the 92.4mm length. And there is little difference between the two, and the stress of 40mm length reinforcement is small, which is not easy to destroy.

Therefore, when the height of the reinforcement is 40mm, the length is 40mm, and the thickness is between 30mm and 40mm, it is the composite working condition.

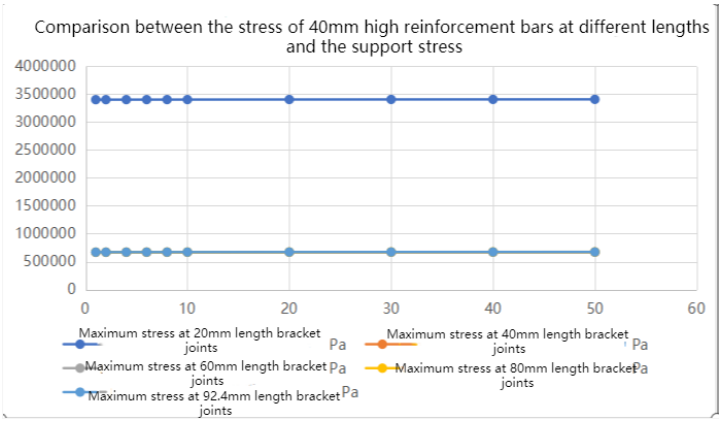

(a)Comparison between the stress of 40mm high reinforcement bars at different lengths and the support stress

ISSN: 2664-9640

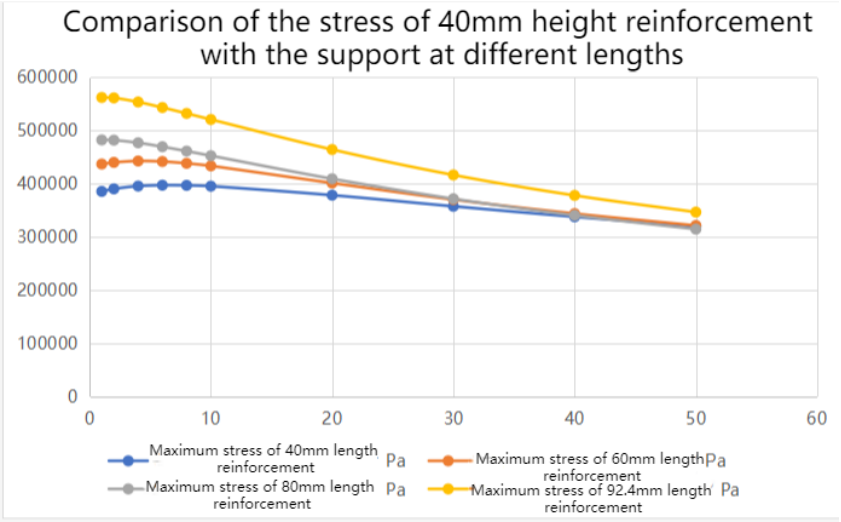

(b)Comparison of the stress of 40mm height reinforcement with the support at different lengths

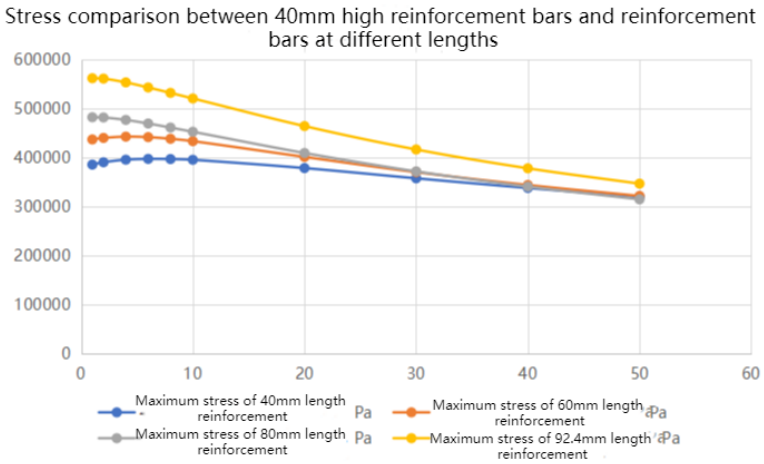

(c)Stress comparison between 40mm high reinforcement bars and reinforcement bars at different lengths

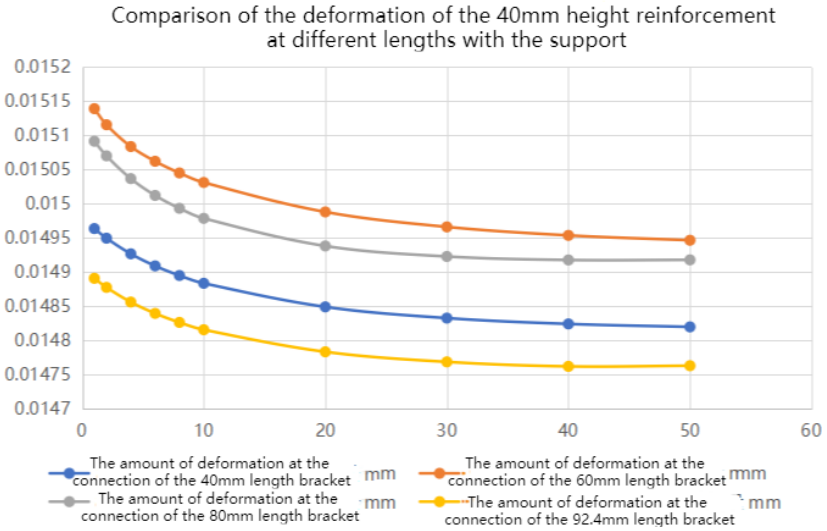

(d)Comparison of the deformation of the 40mm height reinforcement at different lengths with the support

ISSN: 2664-9640

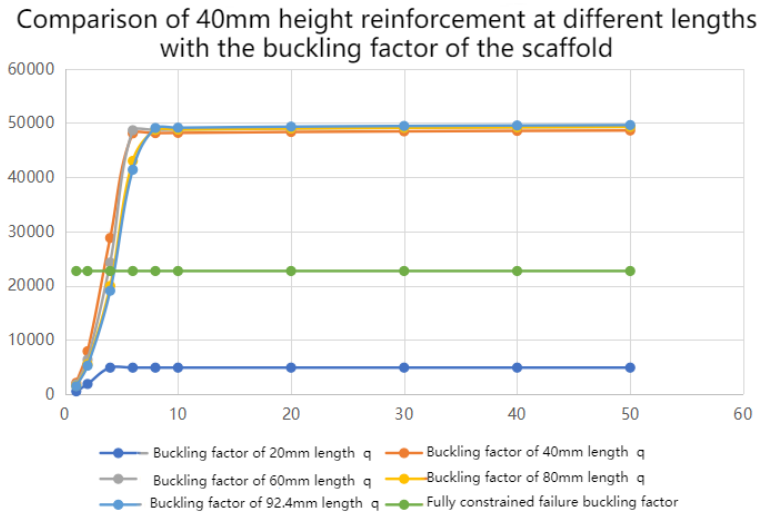

(e) Comparison of 40mm height reinforcement at different lengths with the buckling factor of the scaffold

Figure 24: Relationship between different heights of 40mm high reinforcement bars and support

It can be seen from Figure25 (a) that when the reinforcement is at the same height of 60mm and the thickness range is 1mm to 20mm, the bracket with 40mm reinforcement is subjected to the minimum stress. As the thickness gradually rises, the minimum support stress is 20mm reinforcement for the thickness of 20mm to 50mm. It can be seen from Figure25 (b) that in the range of stiffener thickness from 1mm to 40mm, the minimum heart change at the joint of the bracket is that the length of the stiffener is 92.4mm, while the length of 20mm stiffener has a large deformation, which is not suitable for selection. Combined with Figure25 (c) and (d), it can be seen that the stress of the 40mm length reinforcement is small, and the deformation at the joint of the support is gradually smaller than that of the 92.4mm length reinforcement after 40mm, and its support stress is second only to that of the 20mm length reinforcement. At the same time, the maximum buckling factor of the 40mm length reinforcement is only smaller than that of the 92.4mm length reinforcement, and the maximum buckling factor of the 92.4mm length reinforcement is when the thickness exceeds 10mm.

Therefore, when the height of the reinforcement is 60mm, the length is 40mm, and the thickness is 8mm to 10mm, the reinforcement in the composite condition can be made at the lowest cost.

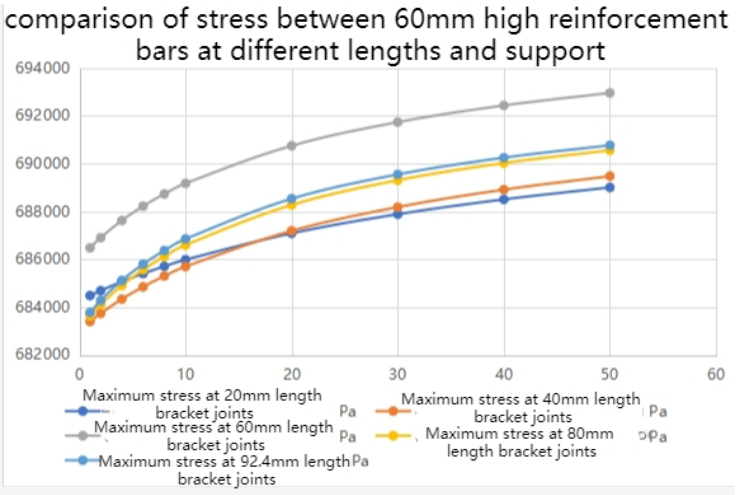

(a)comparison of stress between 60mm high reinforcement bars at different lengths and support

ISSN: 2664-9640

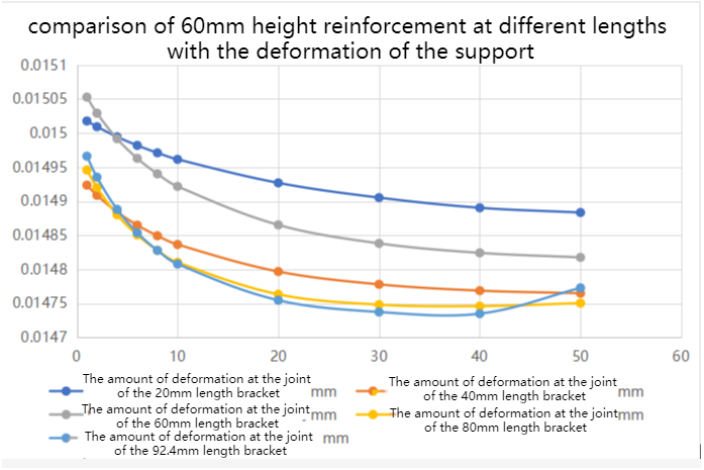

(b)comparison of 60mm height reinforcement at different lengths with the deformation of the support

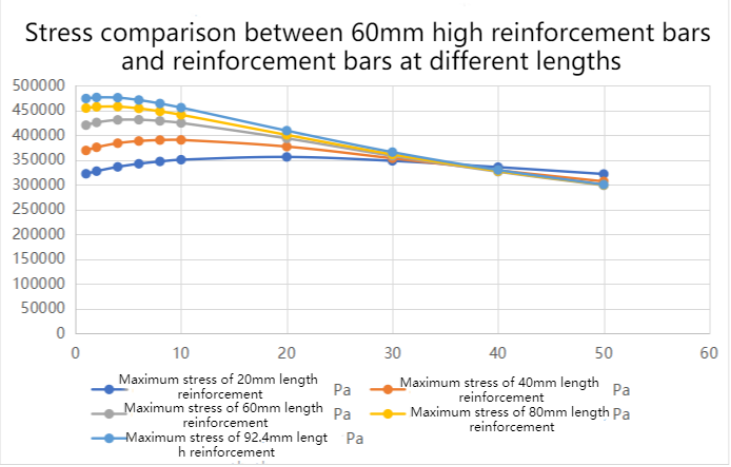

(c)Stress comparison between 60mm high reinforcement bars and reinforcement bars at different lengths

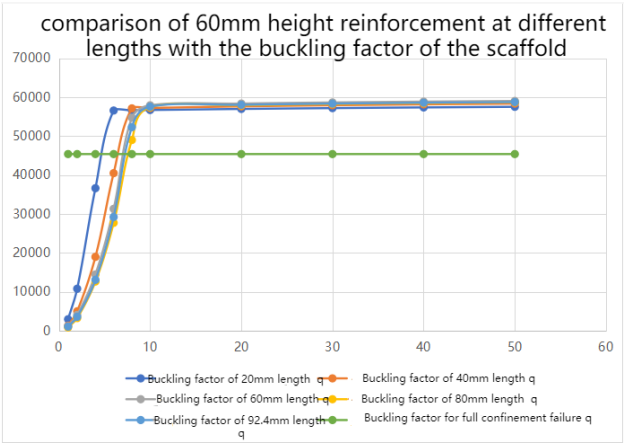

(d) comparison of 60mm height reinforcement at different lengths with the buckling factor of the scaffold

Figure26 Relationship between different heights of 60mm high reinforcement bars and the support

ISSN: 2664-9640

6. Conclusion

In this paper, finite element simulation analysis shows that the stress and deformation at the joint of the support are the largest under the condition of full constraint failure, while the support can still maintain its original function under the condition of single constraint failure, and the upper and lower constraint failure under the condition of double constraint failure has the deformation and stress close to that under the condition of full constraint failure. In order to resist the deformation of the bracket under full constraint failure, stiffeners are added at the joint to resist the large stress and deformation of the constraint failure, and finite element simulation is used to study the height, length and thickness of the stiffeners. It can be known that (1) when the height of the stiffeners is 60mm, the length is 40mm and the thickness is 8mm to 10mm, Its deformation is 0.014750501mm; (2) when the height of the reinforcement is 40mm, the length is 40mm, and the thickness is between 30mm and 40mm, the deformation is and 0.014832415mm; (3) When the height is 20mm, the length of the reinforcement is 92.4mm, and the thickness is 40mm to 50mm, and the deformation is 0.014909375mm.

References

[1]. Wang C H, Miller K J. Short fatigue crack growth under mean stress, uniaxial loading. Fatigue and Fracture of Materials and Structures, 2006, 16(2): 181-198.
[2]. Dowling N E. Notched member fatigue life prediction combing creat initiation and propagation. Fatigue and Fracture of Materials and Structures 2005, 2(2): 129-138.
[3]. Chen Weigong, Zhai Zhihao, Mei Jixian, Quan Maoyuan. Theoretical Mechanics [M], 5th edition, Beijing: Higher Education Press, 2012.
[4]. Liu Hongwen, Mechanics of Materials [M], 6th edition, Beijing: Higher Education Press, 2014
[5]. Liu Fangkang, Mechanical Vibration, Beijing: Aviation Industry Press, 2000.
[6]. Huang Yongqiang, Chen Shuxun, Theory of Mechanical Vibration, Beijing: Machinery Industry Press, 2006.
[7]. Wang Fengquan, Zheng Wangan, Experimental Vibration Analysis, Nanjing: Jiangsu Science and Technology Press, 1998.
[8]. Zhang Ziming, Du Chengbin, Structural Dynamics, Nanjing, Hohai University Press, 2001.